“Centenary commemoration of the discovery of the Evershed effect”

Magnetic Coupling between the Interior and the Atmosphere of the Sun

Magnetic coupling in the quiet solar atmosphere

O. Steiner

1. The quiet Sun magnetic field

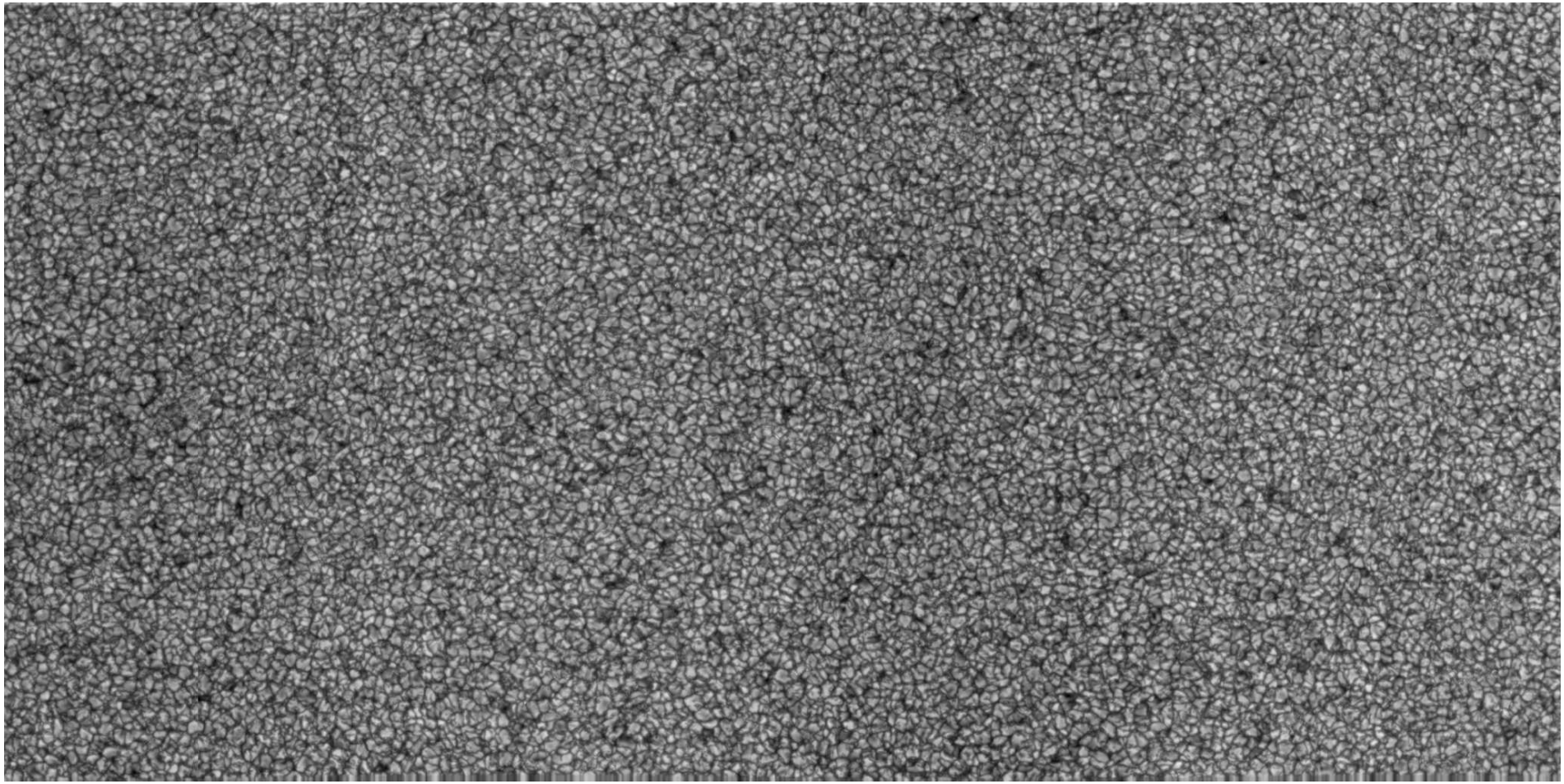

Continuum intensity at 630 nm over a field of view of $302'' \times 162''$. From *Lites et. al. 2008, ApJ 672, 1237*

The quiet Sun magnetic field (cont.)

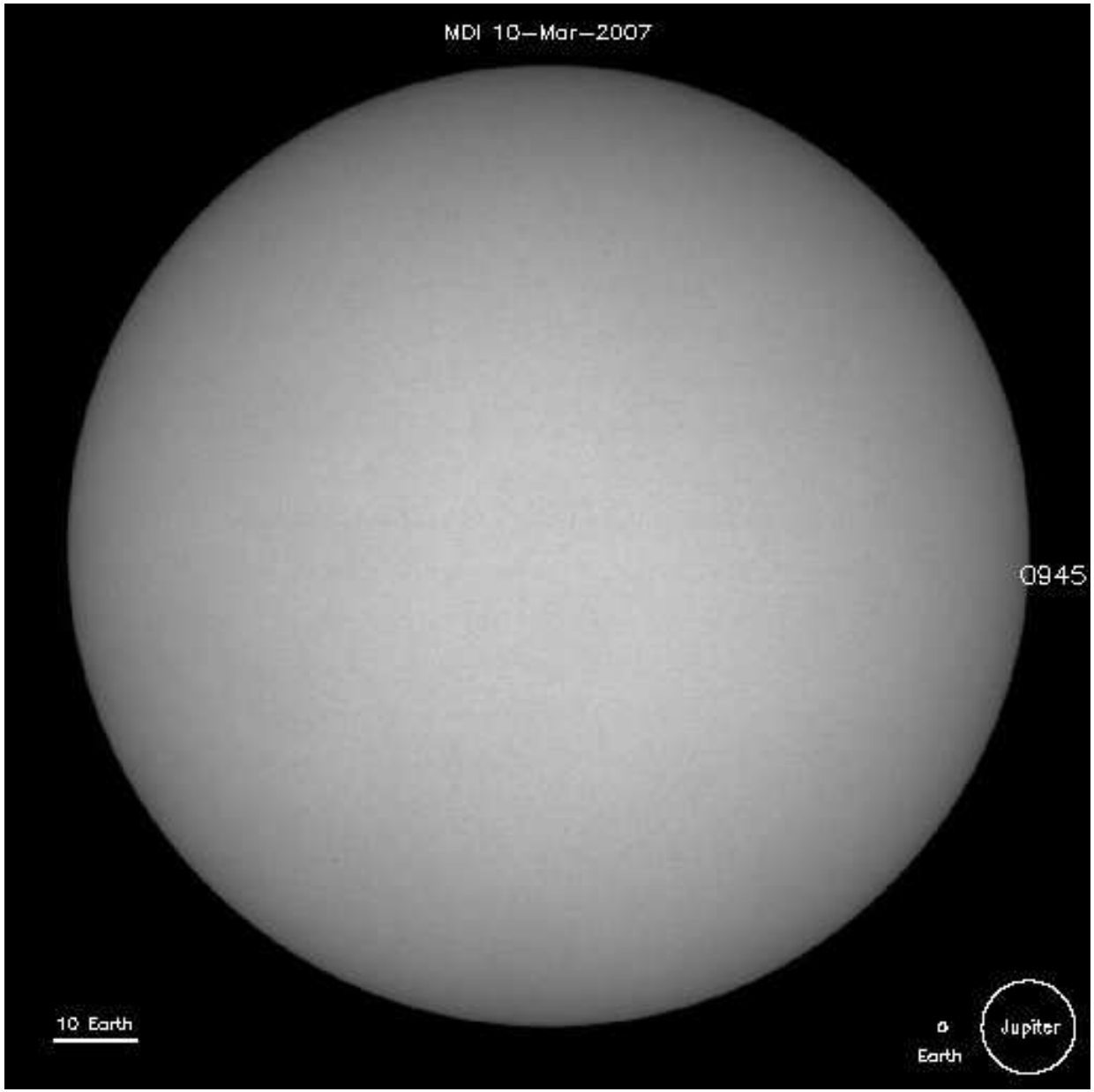

The quiet Sun magnetic field (cont.)

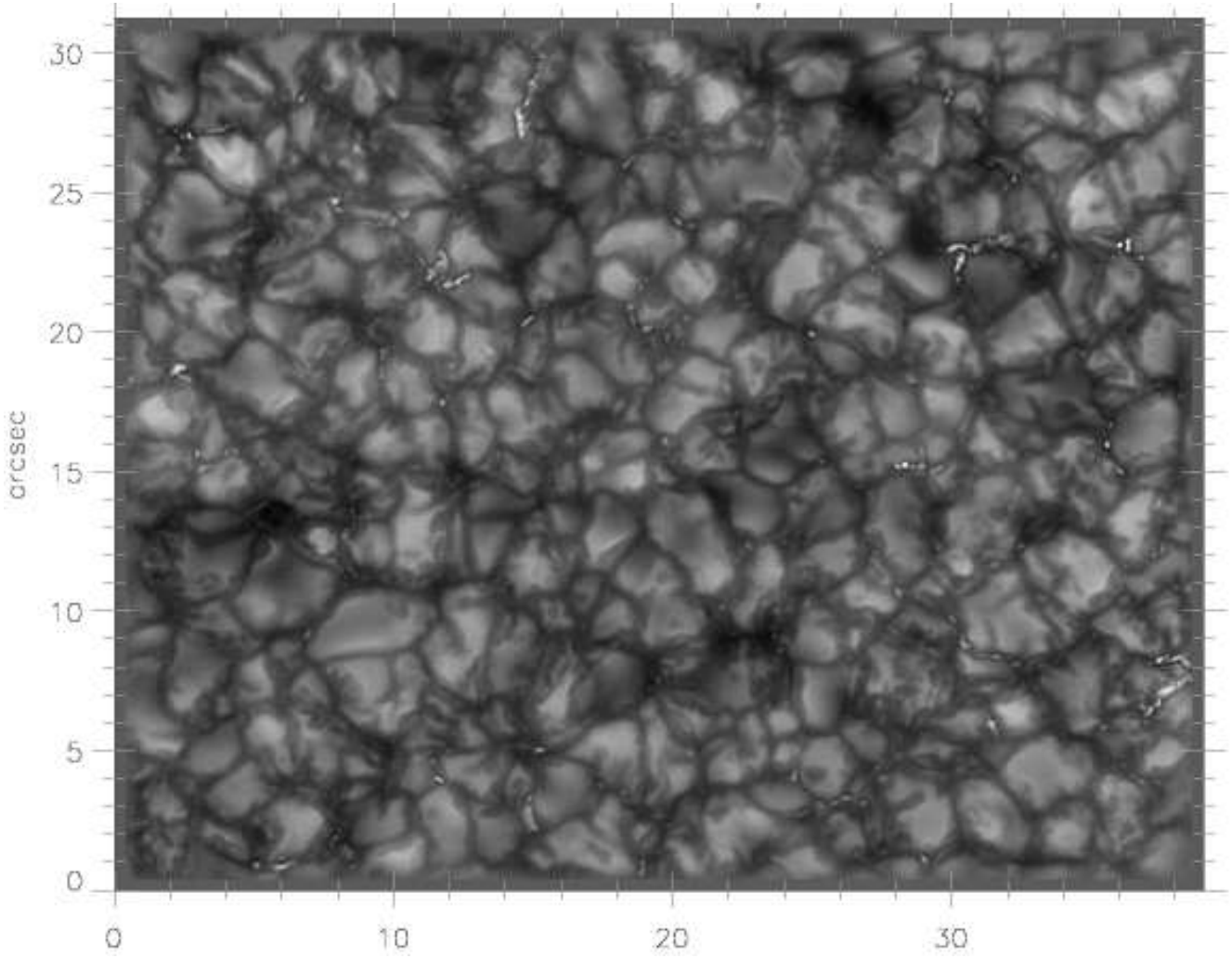

Continuum at 395 nm with the VTT and KAOS at Tenerife

The filigree *Dunn & Zirker, 1973*

Facular points *Mehltretter, 1973*

G-band bright points

Ribbon bands, Flowers etc.

Berger et al. 2006

The quiet Sun magnetic field (cont.)

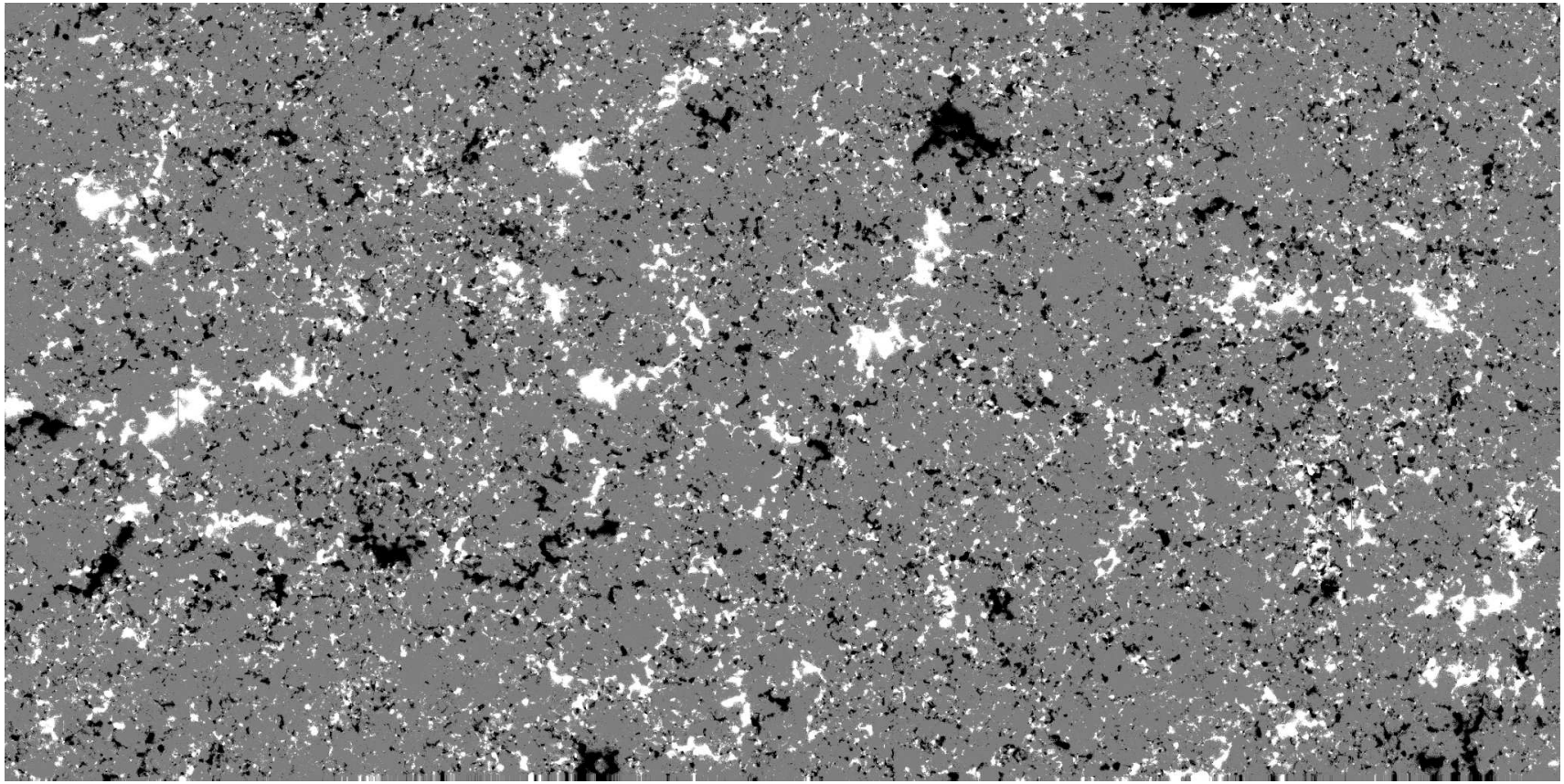

Apparent vertical magnetic flux density, $B^{\rm L}_{\rm app}$, of the quiet Sun over a field of view of $302'' \times 162''$. The grey scale saturates at ± 50 Mx cm^{-2}. 2048 steps to 5 s.

$\langle |B^{\rm L}_{\rm app}| \rangle = 11.7$ *Mx cm*$^{-2}$. From *Lites et. al. 2008, ApJ 672, 1237*

The quiet Sun magnetic field (cont.)

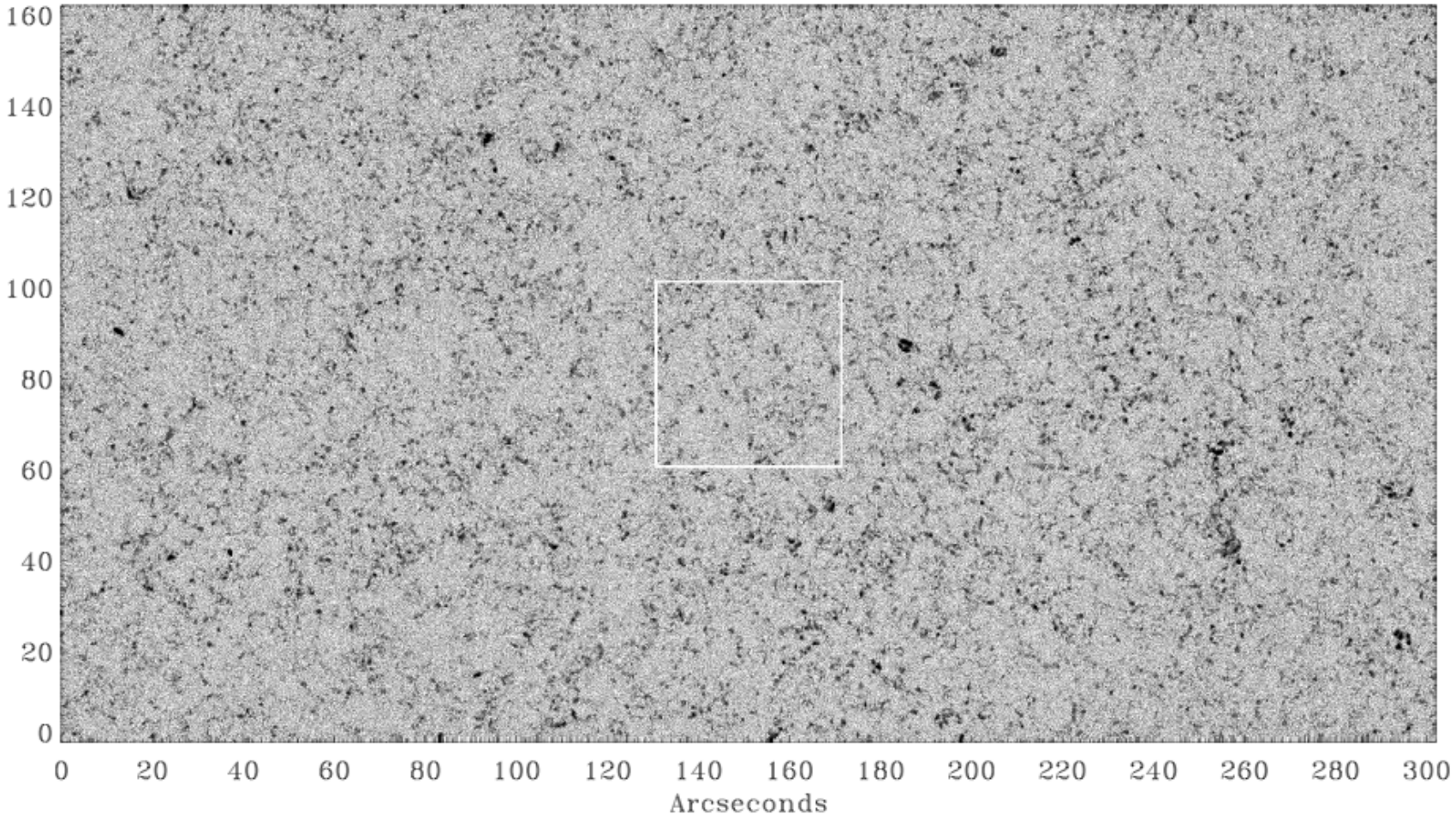

Apparent horizontal magnetic flux density, $B^{\rm T}_{\rm app}$, of the quiet Sun over a field of view of $302'' \times 162''$. The grey scale saturates at ± 200 Mx cm^{-2}. 2048 steps to 5 s.

$\langle B^{\rm T}_{\rm app} \rangle = 60.0$ *Mx cm*$^{-2}$. From *Lites et. al. 08*

The quiet Sun magnetic field (cont.)

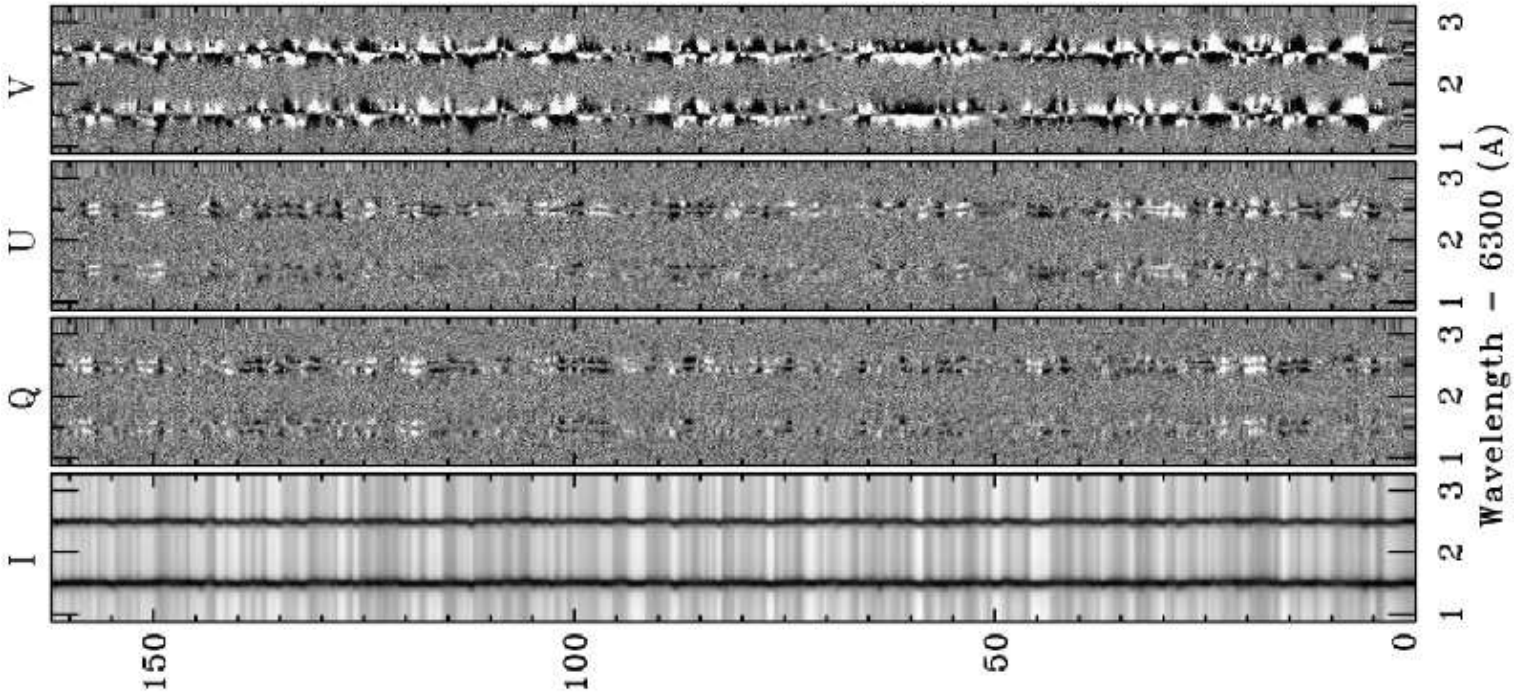

Deep mode *Stokes spectra* with an integration time of 67.2 s and a rms polarization in the continuum of 3×10^{-4}. From a 2-hour time series Lites et al. obtain mean apparent longitudinal and transversal field strengths of $\langle B^{\rm L}_{\rm app} \rangle = 11.0$ Mx cm^{-2} and $\langle B^{\rm T}_{\rm app} \rangle = 55.3$ Mx cm^{-2}. From *Lites et al. 08*

The quiet Sun magnetic field (cont.)

A predominance of horizontally directed magnetic fields in the quiet Sun was also reported by *Orozco Suárez et al. 07* from *HINODE* measurements and by *Harvey et al. 07* from center-to-limb measurements with GONG and SOLIS.

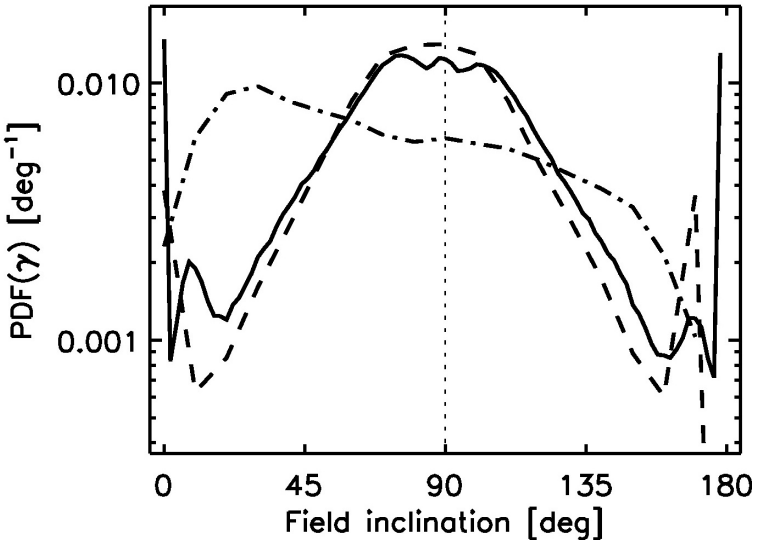

Probability density of the magnetic field inclination in the inter-network. From *Orozco Suárez et al. 07*.

Ishikawa et. al. 08 detected transient horizontal magnetic fields in plage regions with SOT/HINODE

Previously, *Meunier et al. 1998* and *Martinez Pillet et al. 97* reported observations of weak and strong horizontal field in quiet Sun regions.

Questions:

- Do simulations of the surface layers of the Sun intrinsically produce horizontal magnetic fields ?
- If yes, how do they originate ?
- How does the polarimetric signal from simulations compare to measurements ?

Schüssler & Vögler 2008, A&A 481, L5-L8

Steiner, Rezaei, Schaffenberger, and Wedemeyer-Böhm 2008, ApJ 680, L85-L88

Grossmann-Doerth et al. 1998 noted: “we find in all simulations also strong horizontal fields above convective upflows”

2. Coupling convection–magnetic field

Three-dimensional computational domain encompassing the integral layers from the upper convection zone to the middle chromosphere.

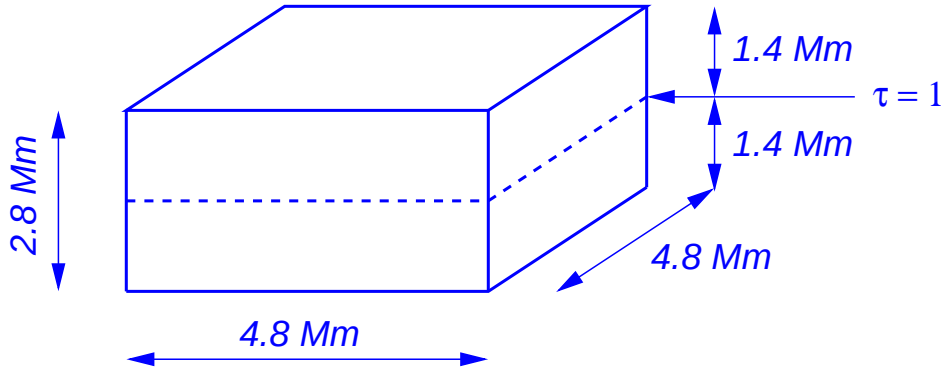

Top boundary located sufficiently high for not to unduly tamper the photospheric layers, from where the polarimetric signals measured with SOT/Hinode originate.

Two simulation runs, which significantly differ in their initial and boundary conditions for the magnetic field.

Coupling convection–magnetic field (cont.)

Different initial states and boundary conditions for the magnetic field

v10

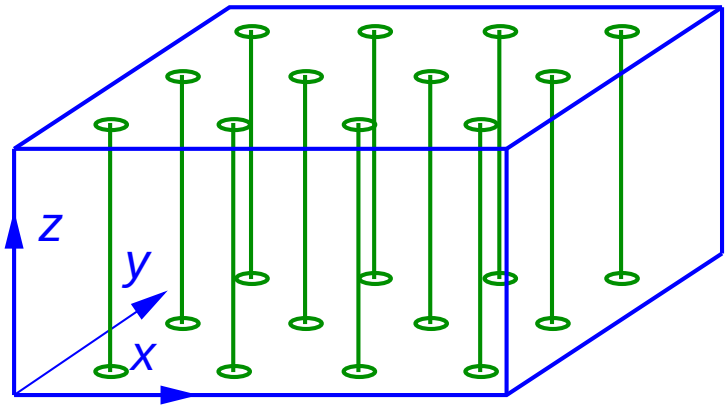

Initial homogeneous, vertical, unipolar **B**-field of 10 G.

$B_{x,y} = 0; \quad \partial B_z / \partial z = 0$

h20

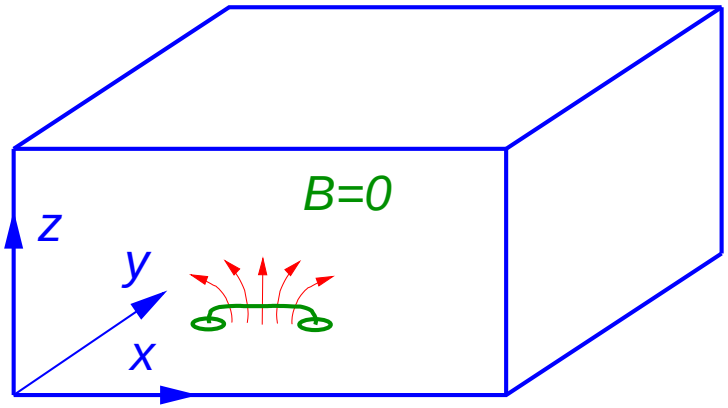

Fluid that enters the simulation domain from below carries horizontal magnetic field of $B_x = 20$ G.

$\partial B_{x,y,z} \partial z = 0$

Coupling convection–magnetic field (cont.)

Horizontally and temporally averaged absolute vertical and horizontal magnetic flux density as a function of height for both runs.

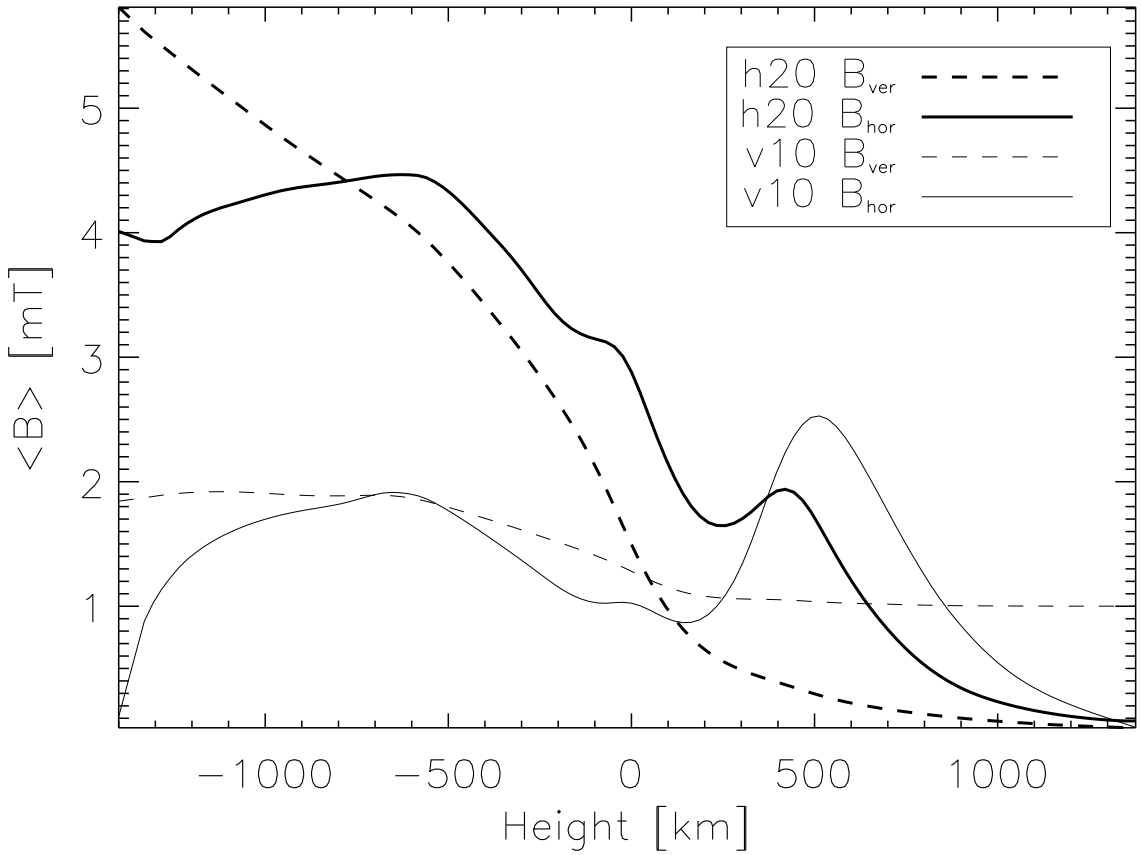

$$\langle B_{\rm hor}\rangle = \langle\sqrt{B_x^2 + B_y^2}\,\rangle$$

run v10:

$$\langle B_{\rm hor}\rangle / \langle |B_{\rm ver}|\rangle (500\,\text{km}) = 2.5$$

run h20:

$$\langle B_{\rm hor}\rangle / \langle |B_{\rm ver}|\rangle (420\,\text{km}) = 5.6$$

Coupling convection–magnetic field (cont.)

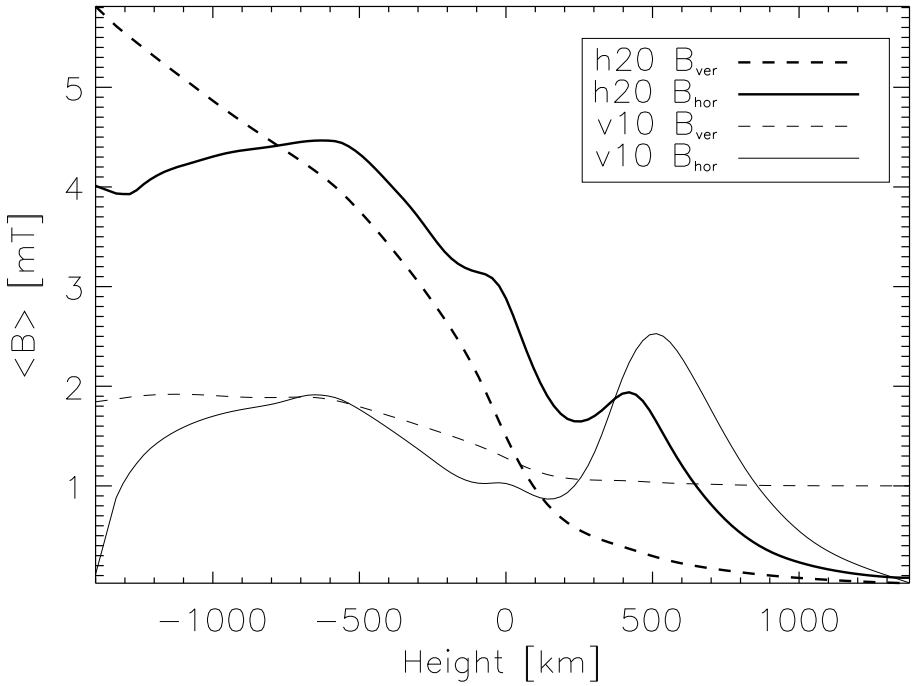

$\langle B_{\rm hor} \rangle$ (———-) and $\langle B_{\rm ver} \rangle$ (– – – – –) as a function of height z for run h20 (heavy) and run v10 (thin).

From *Steiner et al. 2008*

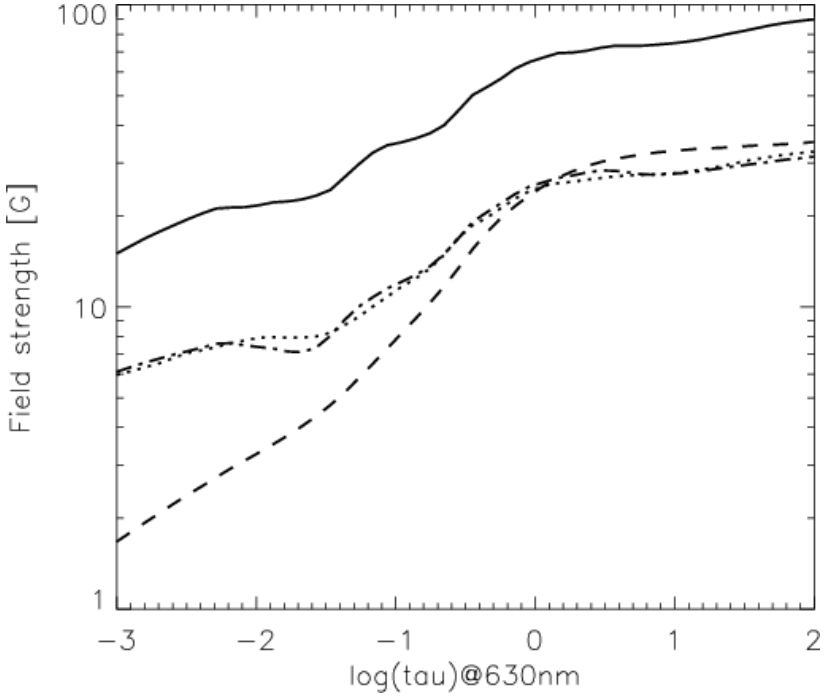

$\langle B_x \rangle$ (— · — · — · —), $\langle B_y \rangle$ (. . . . . .), and $\langle B_{\rm ver} \rangle$ (- - - -) as a function of $\log \tau_{630\ \rm nm}$.

From *Schüssler & Vögler 2008*

Coupling convection–magnetic field (cont.)

Probability density functions of the magnetic field inclination from *observations of Orozco Suárez et al. (2007)* and simulations

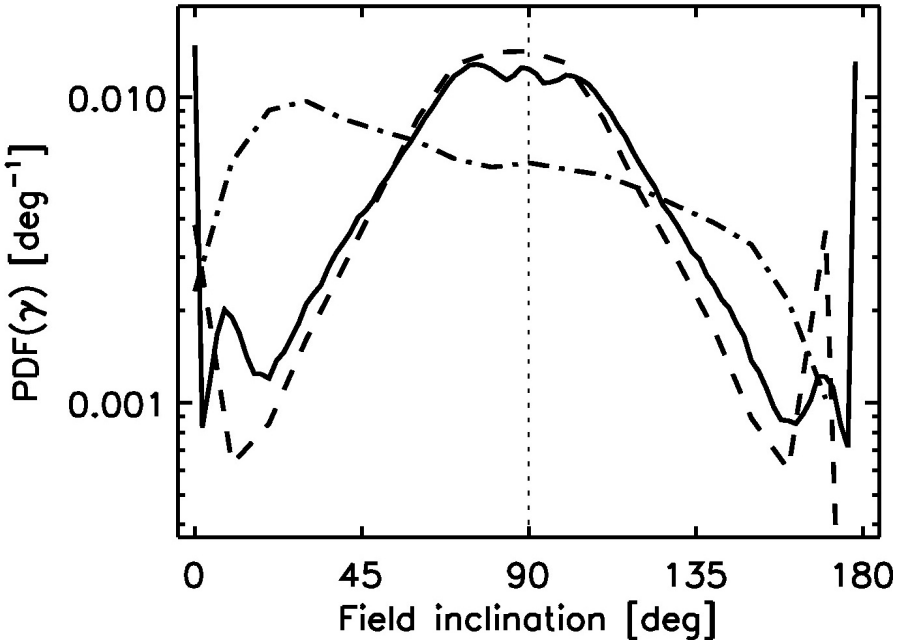

Solid and dashed PDFs represent all pixels in the FOV and the IN regions, respectively. Dot-dashed curve shows PDFs from magnetoconvection *simulations* with a mean flux density of 10 Mx cm^{-2} from *Vögler et al. (2005)*.

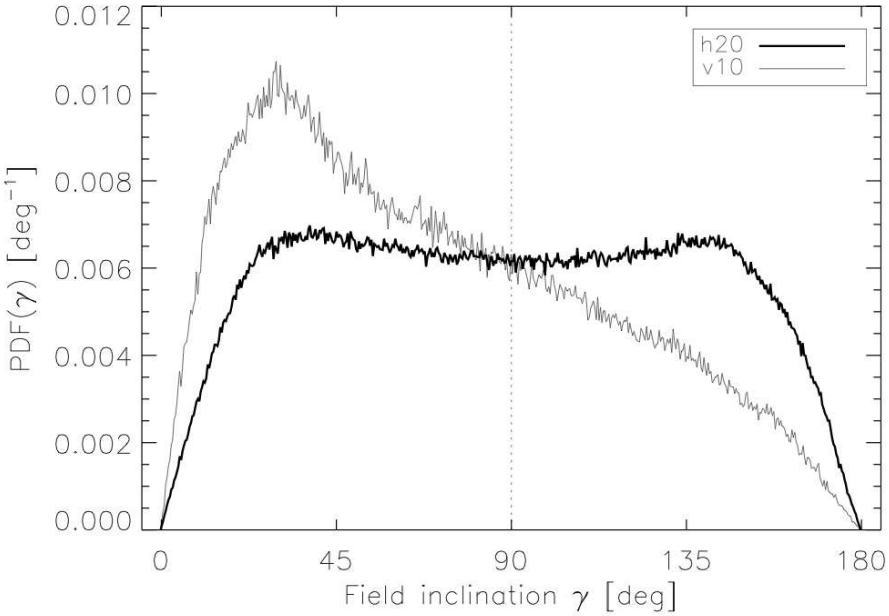

PDF of inclination angle for *simulation* runs h20 and v10 of *Steiner et al. (2008)*.

Coupling convection–magnetic field (cont.)

Vertical section through computational domain...

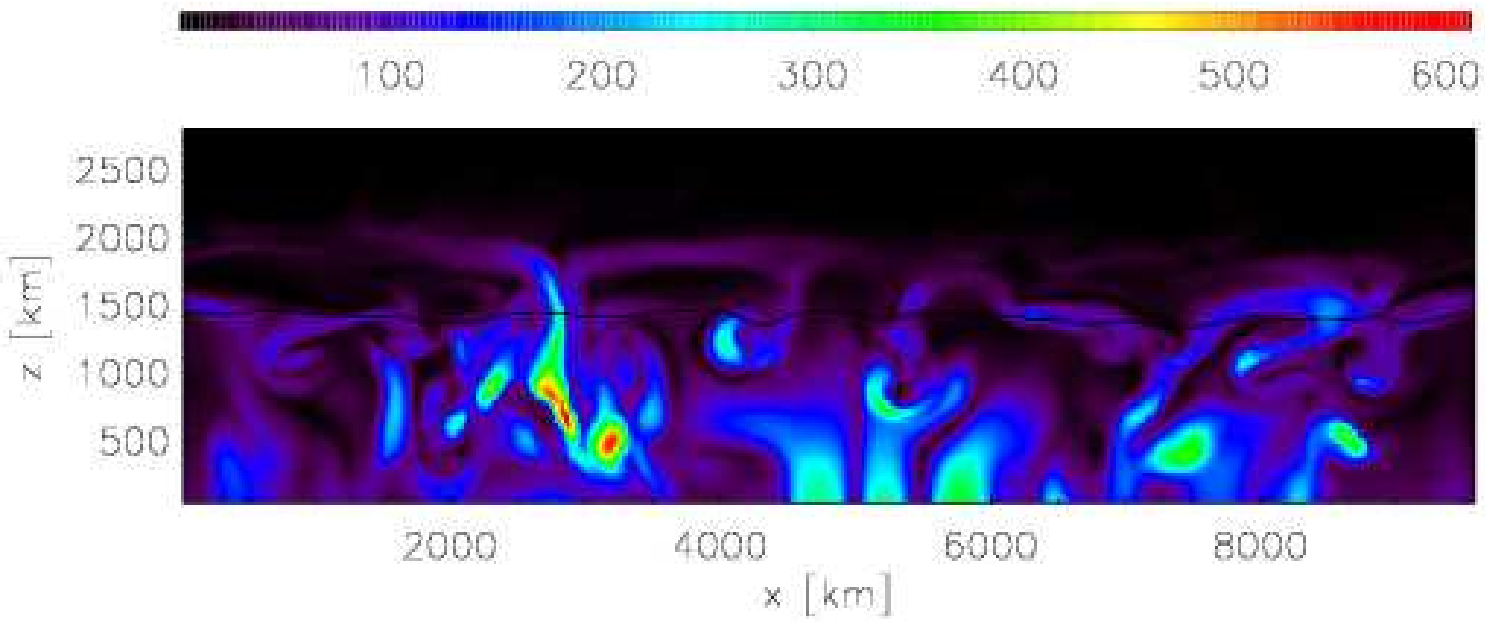

... shows horizontal sheets of enhanced magnetic field strength in the upper photosphere — *the seething magnetic field*. → T movie

Coupling convection–magnetic field (cont.)

Snapshot of $B_{\rm hor}$, $B_{\rm ver}$, and the continuum intensity at 630 nm from *run h20* in the horizontal section of $\langle \tau_{500\,\rm nm} \rangle = 1$.

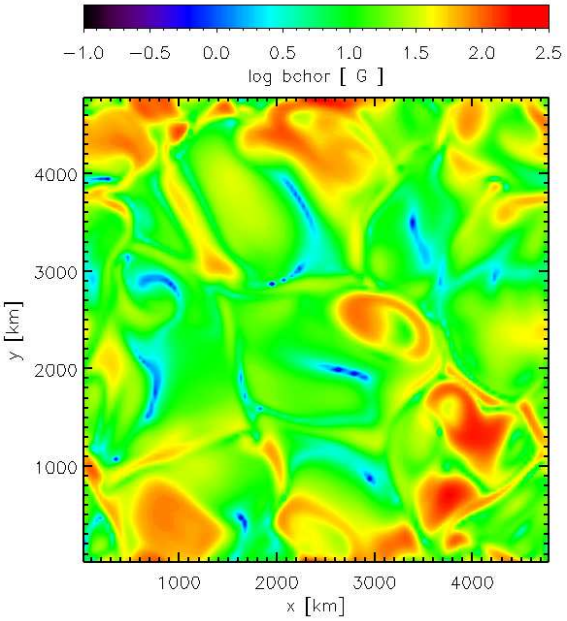

$B_{\rm hor}$

area fraction with

$B_{\rm hor} > 5$ mT $= 17\%$

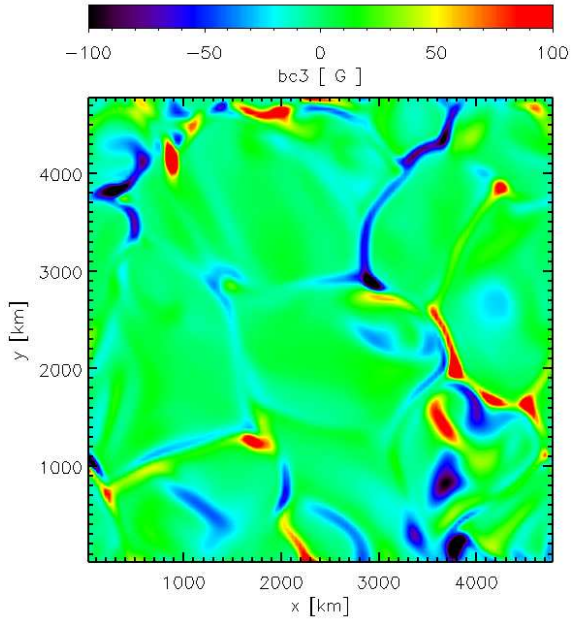

$B_{\rm ver}$

area fraction with

$B_{\rm ver} > 5$ mT $= 2.2\%$

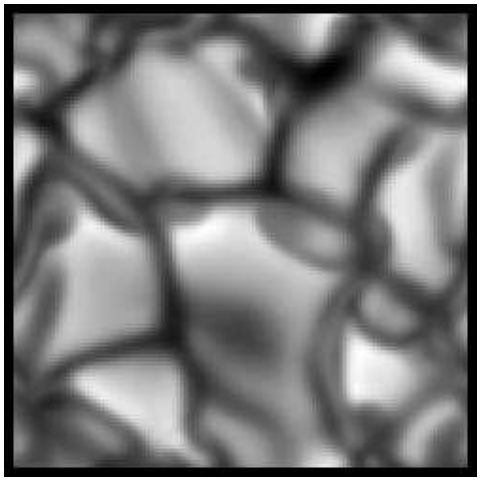

$I_{630\,\rm nm}$

$v_z\,(\langle \tau_{500\,\rm nm} \rangle = 1)$

Movie

Coupling convection–magnetic field (cont.)

The horizontal field can be considered a consequence of the *flux expulsion process* (Parker, 1963; Weiss, 1964): in the same way as magnetic flux is expelled from the granular interior to the intergranular lanes, it also gets pushed to the middle and upper photosphere by overshooting convection, where it tends to form a layer of horizontal field.

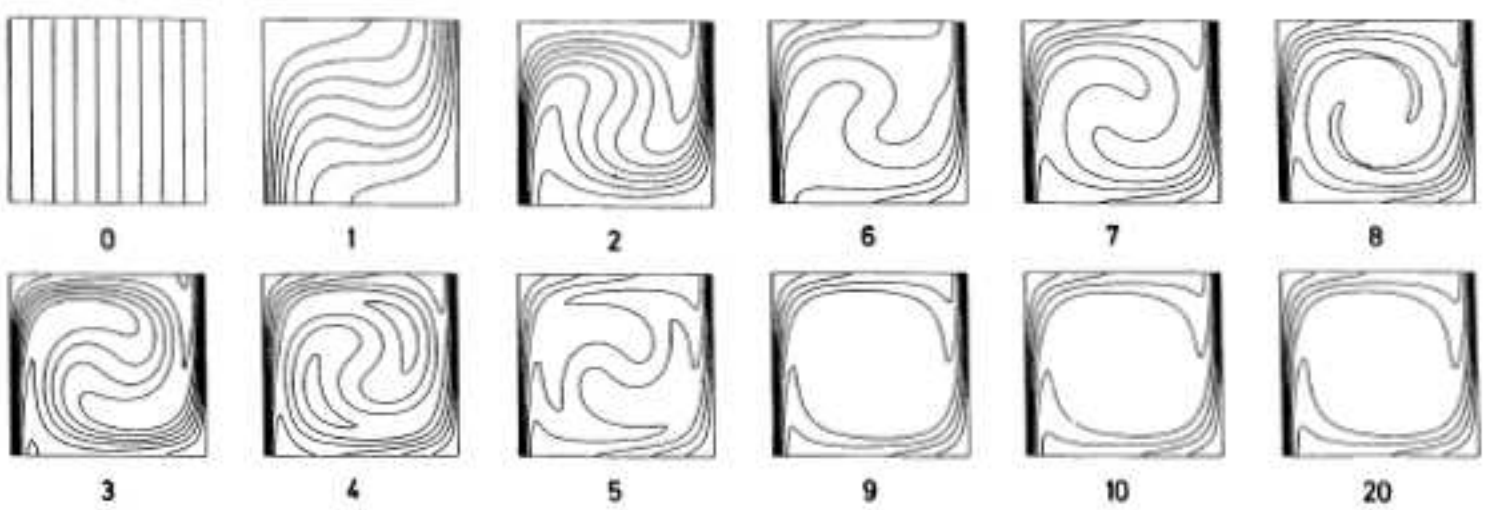

From *Galloway & Weiss, 1981*

Coupling convection–magnetic field (cont.)

Vertically directed Poynting flux, $\langle S_z \rangle$, $\langle B_{\rm hor} \rangle$, and $\langle |B_z| \rangle$ as a function of time and height in the atmosphere. $\mathbf{S} = \frac{1}{4\pi}(\mathbf{B} \times (\mathbf{v} \times \mathbf{B}))$

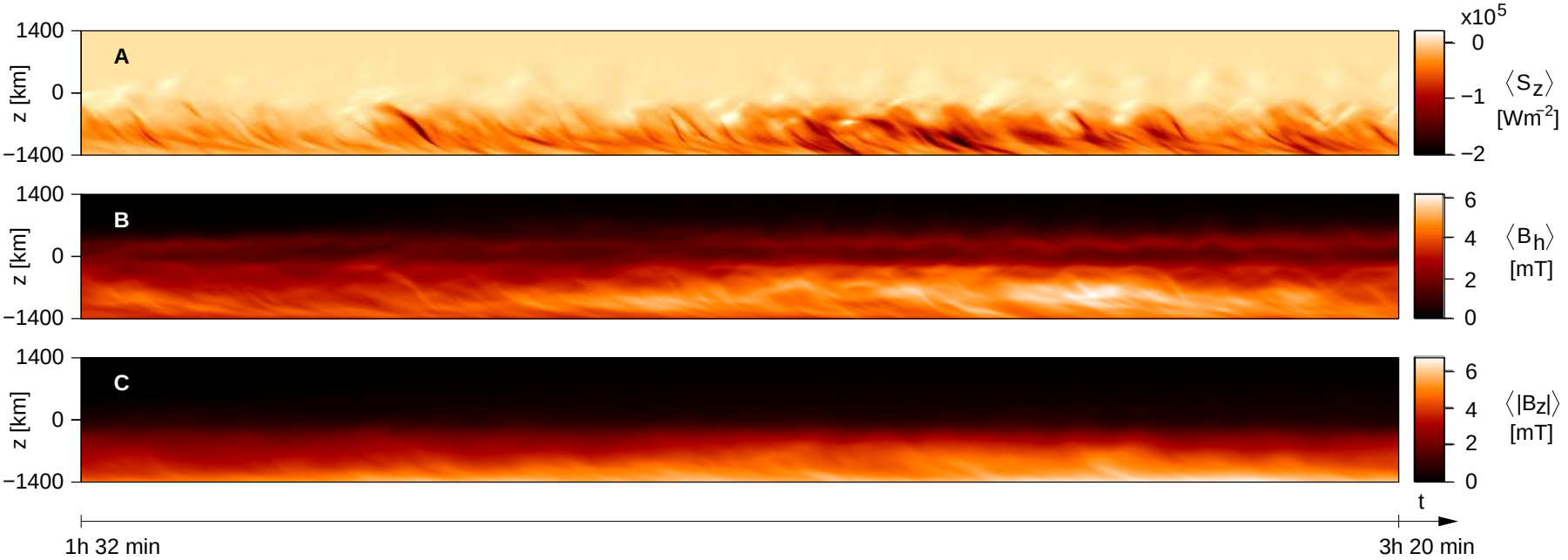

From Steiner, Rezaei, Schaffenberger, & Wedemeyer-Böhm, 2008, ApJ 680, L85-L88

The surface of optical depth unity is a separatrix for the vertically directed Poynting flux.

$$\frac{\partial}{\partial t}\left(\frac{B^2}{8\pi}\right) = -\nabla \cdot (\mathbf{E} \times \mathbf{B}) - \mathbf{u} \cdot (\mathbf{j} \times \mathbf{B}) - Q_{\rm res}$$

Coupling convection–magnetic field (cont.)

The dominance of the horizontal field “results from the intermittent nature of the dynamo field with polarity mixing on small scales in the surface layers”.

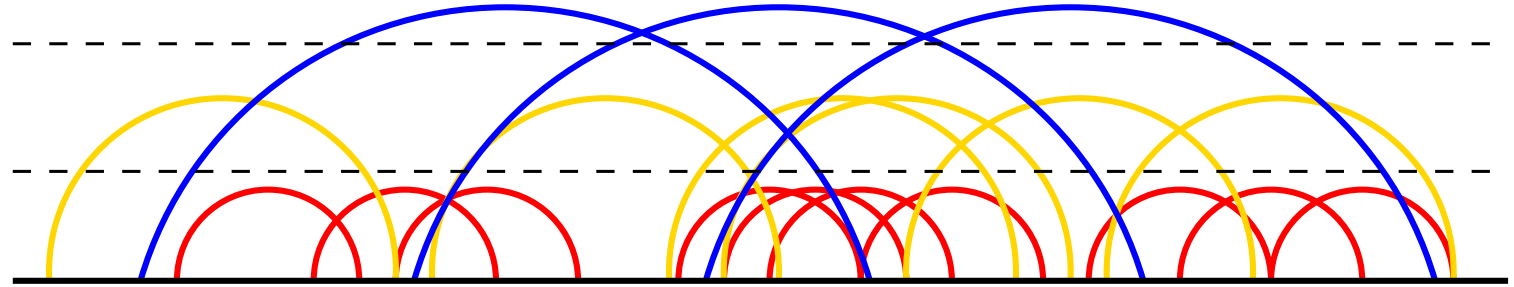

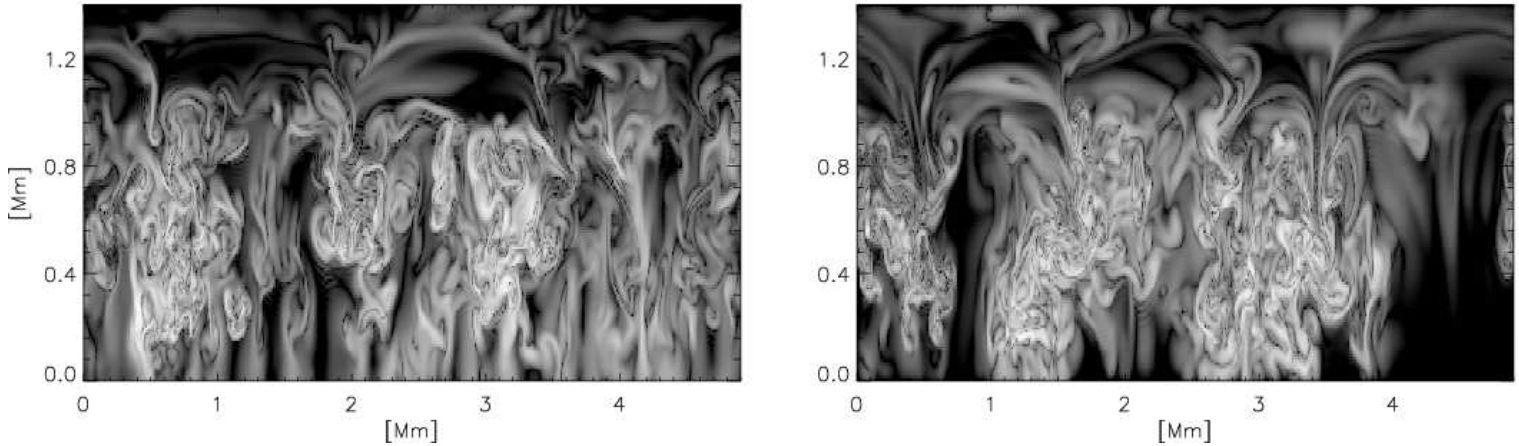

From *Schüssler & Vögler 2008*

Coupling convection–magnetic field (cont.)

Detached horizontal field as a consequence of magnetic reconnection

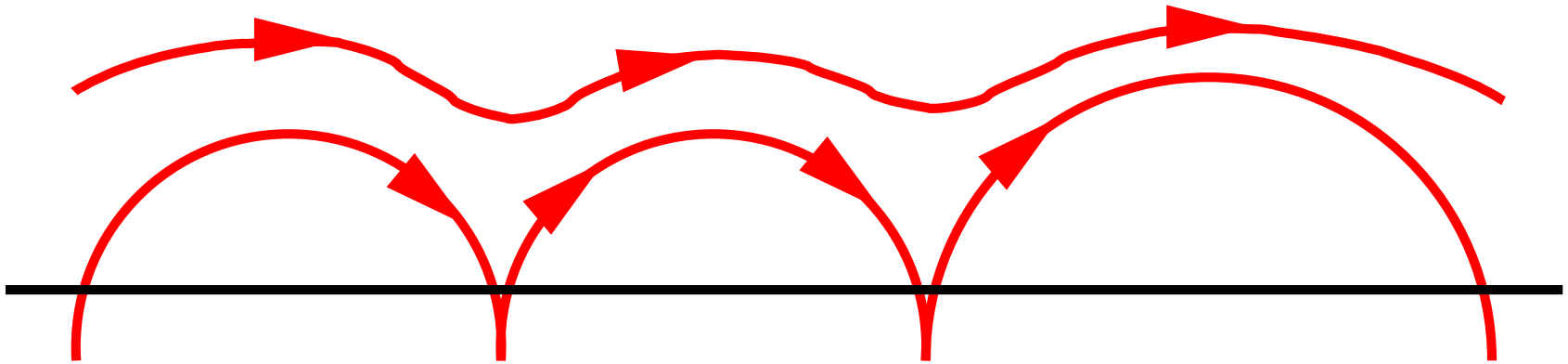

Coupling convection–magnetic field (cont.)

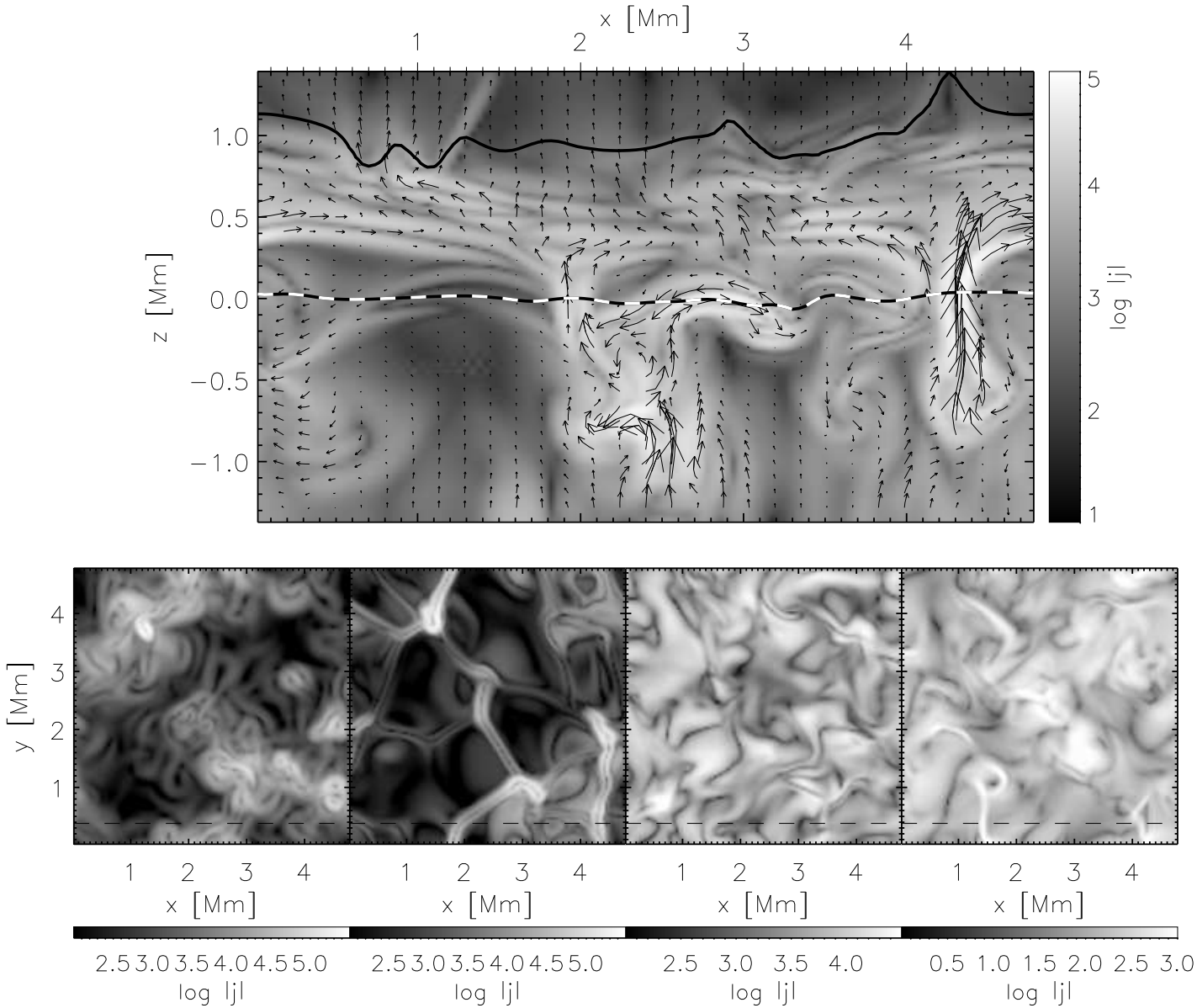

Logarithmic current density, $\log |j|$, in a vertical cross section (top panel) and in four horizontal cross sections in a depth of 1180 km below, and at heights of 90 km, 610 km, and 1310 km above the average height of optical depth unity from left to right, respectively. The arrows in the top panel indicate the *magnetic field* strength and direction.

From Schaffenberger, Wedemeyer-Böhm, Steiner, and Freytag, 2006, ASP Conf. Ser., Vol. 354, p. 345

Coupling convection–magnetic field (cont.)

Vertically directed Poynting flux, $\langle S_z \rangle$, as a function of height in the atmosphere.

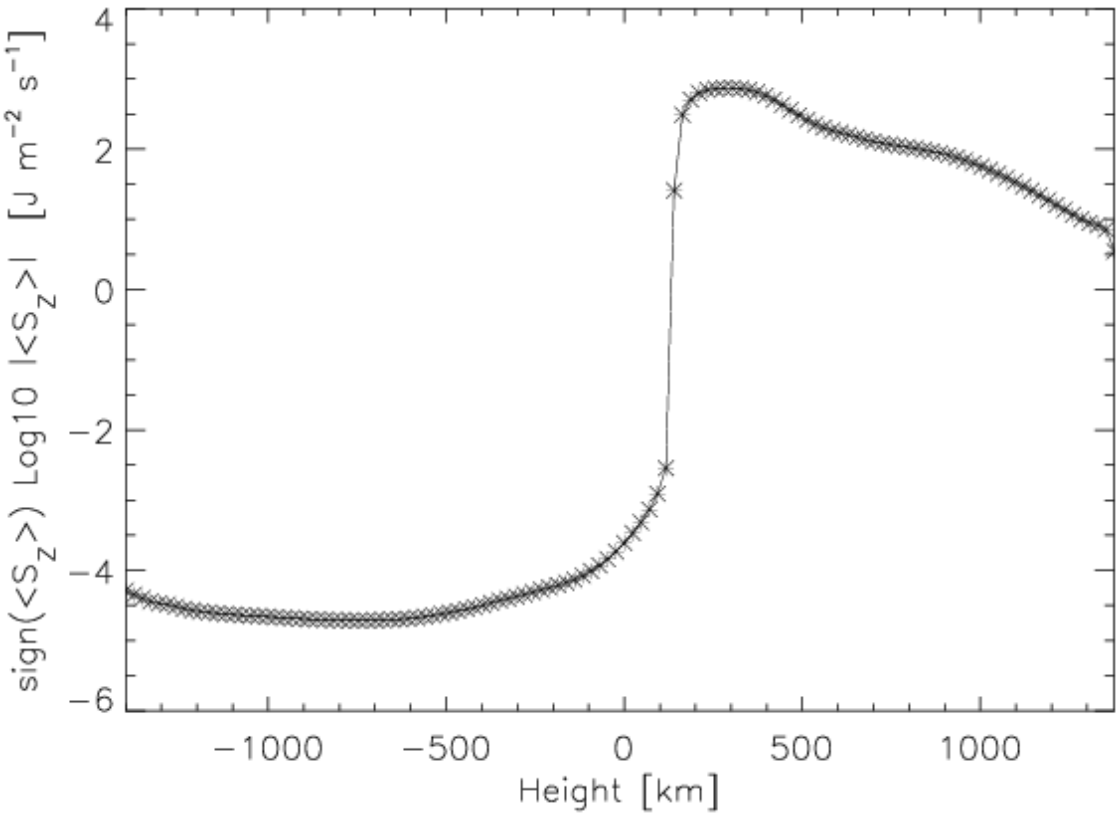

The temporal average of $\langle S_z \rangle$ is maximal 7.4×10^2 Wm^{-2} (at 200 km) and minimal -5.2×10^4 Wm^{-2} (at -800 km). For comparison: the chromospheric radiative energy loss is about 4.3×10^3 Wm^{-2}.

Coupling convection–magnetic field (cont.)

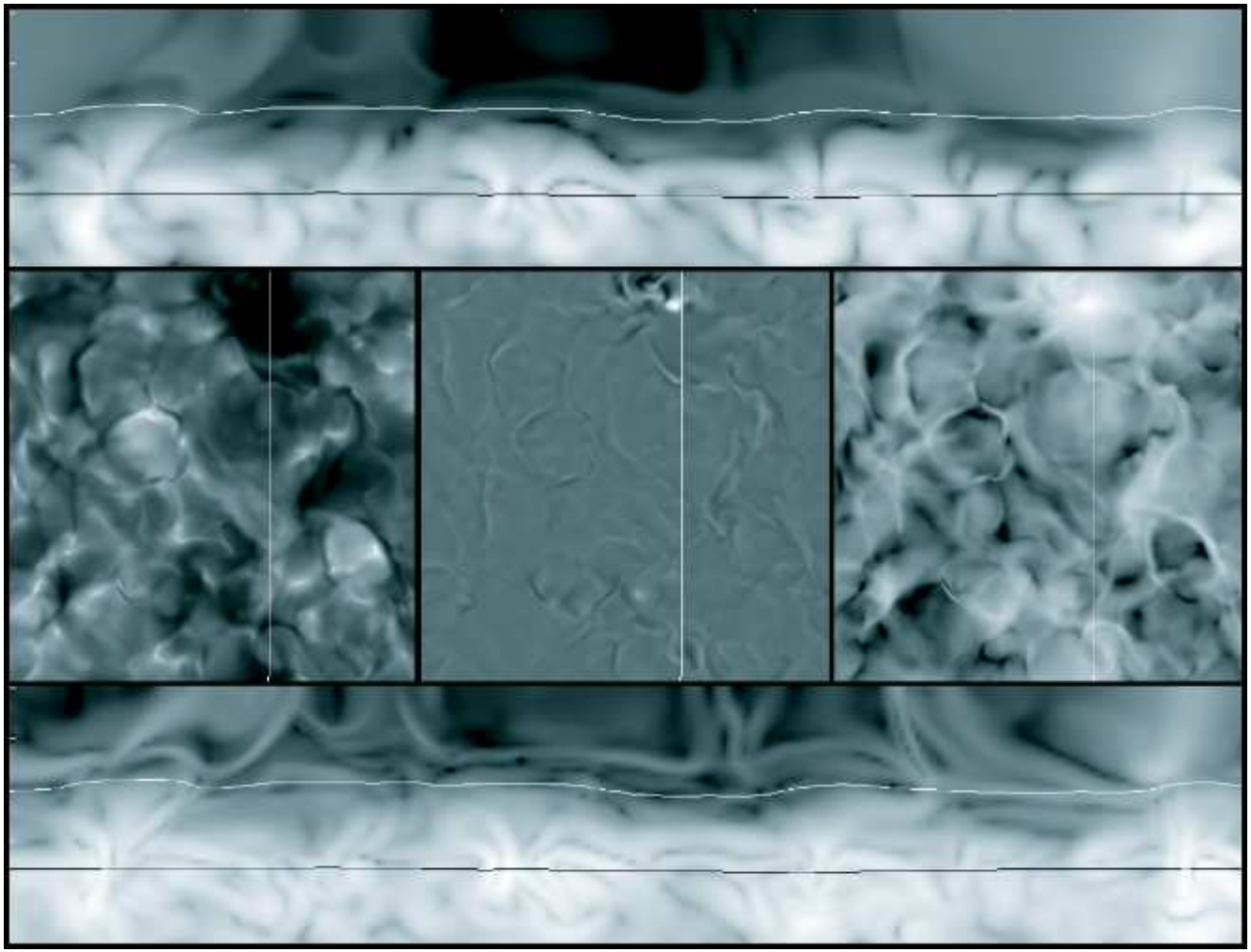

Top: Logarithm of the magnetic field strength. Bottom: Logarithm of the current density.

From *Abbett, ApJ 665, 1469 (2007)*

Coupling convection–magnetic field (cont.)

Recent observational evidences for the “convective collapse” in connection with the formation of magnetic flux concentrations

- Bellot Rubio, L.: 2001, *Observation of Convective Collapse and Upward-moving Shocks in the Quiet Sun*, ApJ, 560, 1010-1019
- Socas-Navarro, H. & Manso Sainz, R.: 2005, *Shocks in the Quiet Solar Photosphere: A Rather Common Occurrence*, ApJ 620, L71-L74
- Nagata et al. 2008 *Formation of Solar Magnetic Flux Tubes with Kilogauss Field Strength Induced by Convective Instability*, ApJ 677, L145-L147
- Shimizu et al. 2008 *Frequent Occurrence of High-Speed Local Mass Downflows on the Solar Surface*, ApJ 680, 1467-1476
- Bello Gonzalez et al.: 2008, *Small-scale magnetic field dynamics on the Sun at high spatial and temporal resolution*, A&A 90, L23-L26
- Fischer, C.E.: 2008, *Analysis of high cadence HINODE SP quiet sun time series*, Hinode II conference
- Danilovic, S. 2008 in prep.

3. Intermezzo

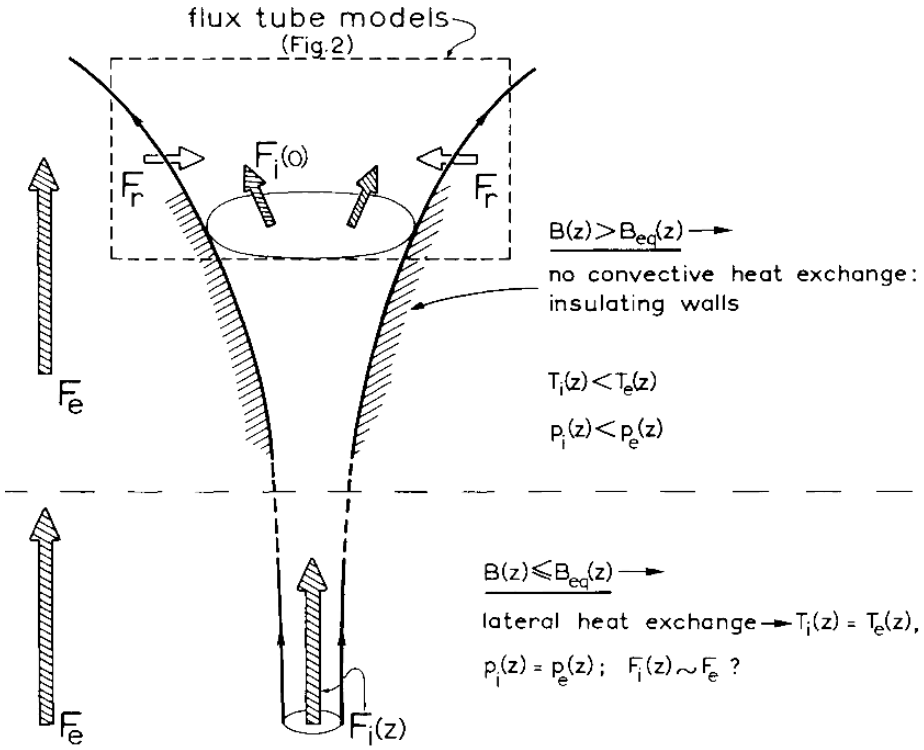

Fig. 5. A quasi-static flux tube with two regimes of heat exchange (schematic).

Magnetic flux tube. *Zwaan, 1978*

3. Intermezzo

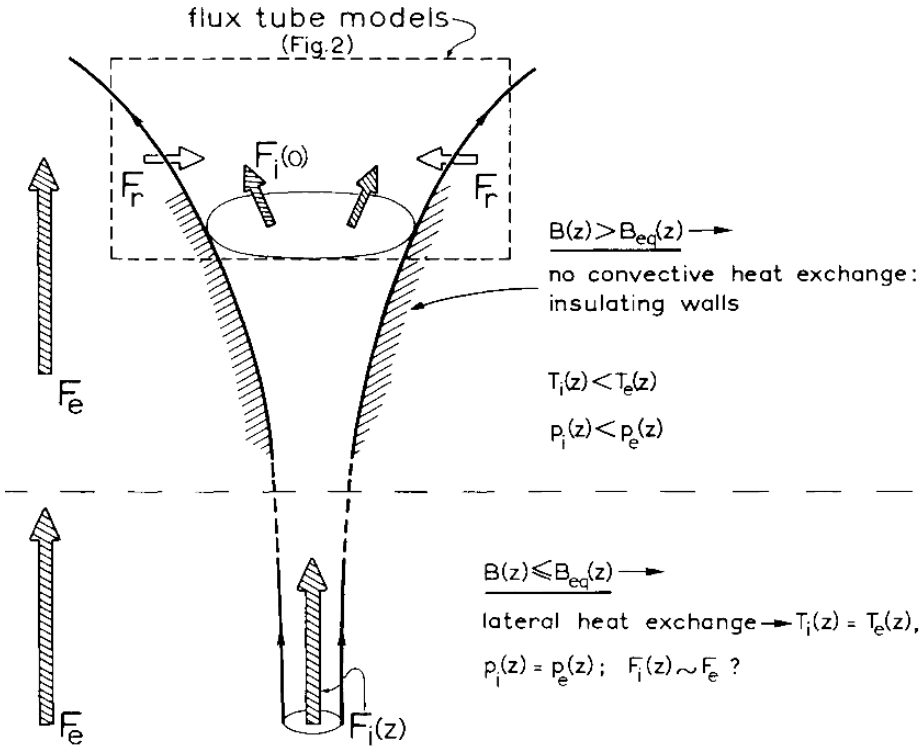

Fig. 5. A quasi-static flux tube with two regimes of heat exchange (schematic).

Magnetic flux tube. *Zwaan, 1978*

"This magnetic-field paradigm has now been shattered...."

Jan Stenflo, 2008, this conference.

3. Intermezzo

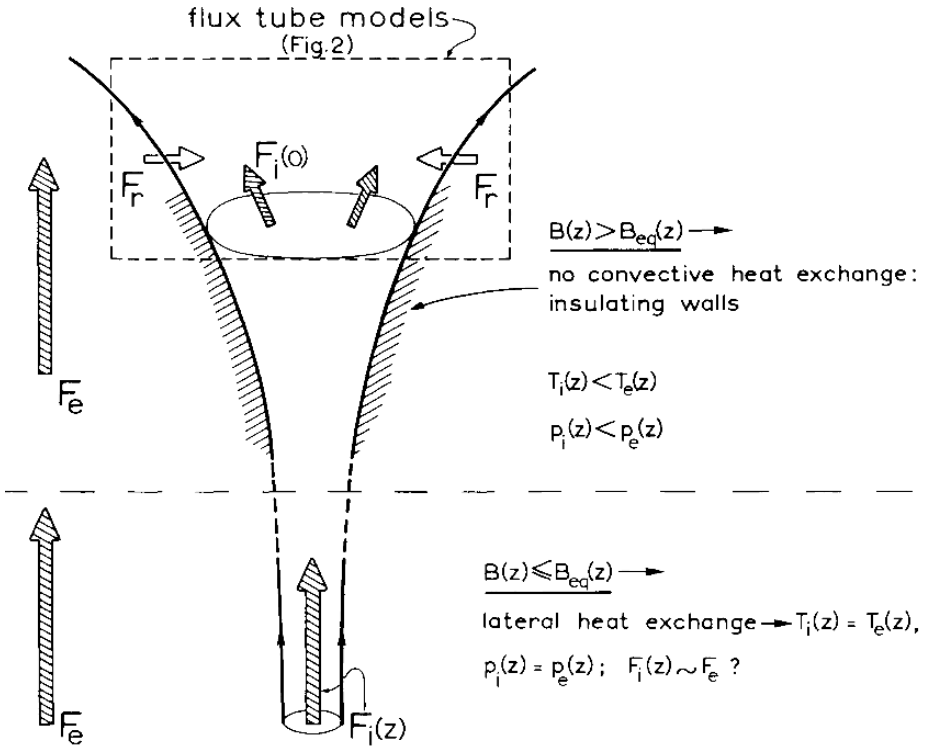

Fig. 5. A quasi-static flux tube with two regimes of heat exchange (schematic).

Magnetic flux tube. *Zwaan, 1978*

"This magnetic-field paradigm has now been shattered...."

Jan Stenflo, 2008, this conference.

"....resolution-independent methods have been developed, showing that *more than 90% of the flux occurs in strong-field form with the kG flux fragments or 'flux tubes'* occupying on the average only a fraction (a few tenths) of one percent of the solar surface."

Stenflo, 1989

Intermezzo (cont.)

Howard & Stenflo [1972, SP 2] found that “more than 90% of the total flux *seen with a 17 by 17 arc sec magnetograph aperture* is channeled through narrow filaments with very high field strength in plages and at the boundaries of supergranular cells.”.

Frazier & Stenflo [1972, SP 27] found the same result with a 2.4 by $2.4''$ magnetograph aperture.

4. Coupling waves–magnetic field

Time sequence of a two-dimensional simulation of magnetoconvection starting with an initial homogeneous vertical magnetic field of 100 G.

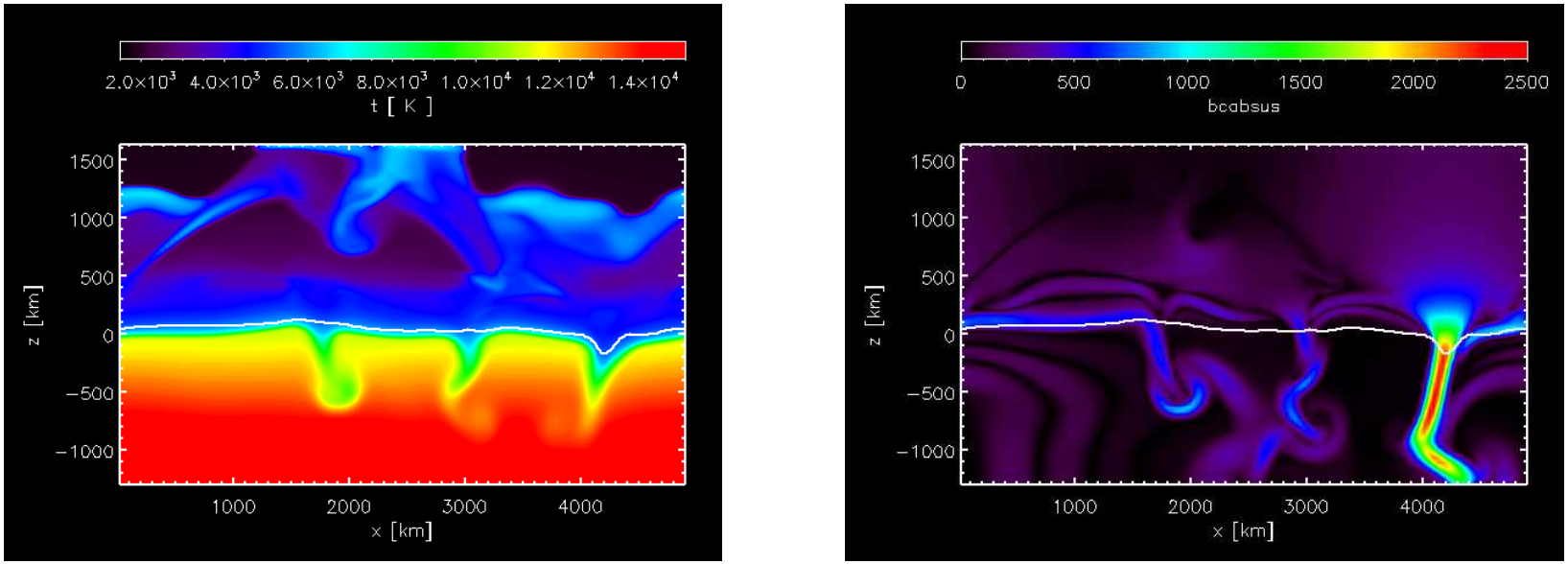

Left: Temperature, *Right:* Absolute magnetic field strength. A magnetic flux sheet has formed at $x \approx 4\,200$ km.

Coupling waves–magnetic field (cont.)

The sequence from $t = 1200$ s to $t = 1450$ s is repeated with a plane parallel, oscillatory velocity perturbation at the bottom boundary with an amplitude of 50 m/s and a frequency of 20 mHz. When subtracting the velocity field of two sequences, the perturbation becomes visible.

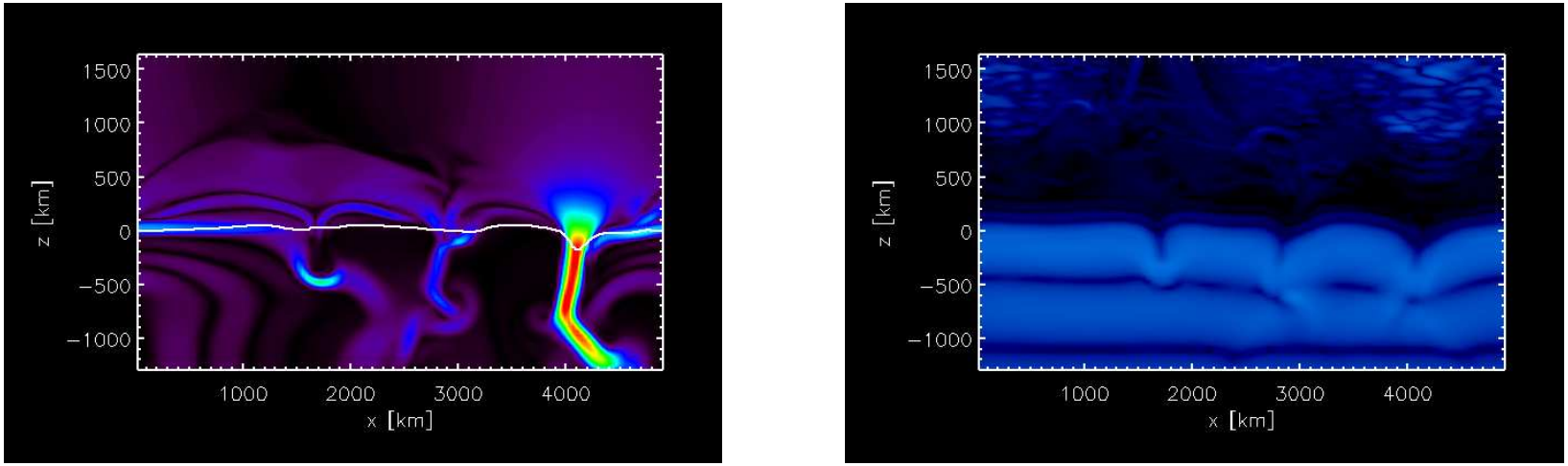

Left: Magnetic field strength. *Right:* Subtractive velocity field 116 s after starting the perturbation.

Coupling waves–magnetic field (cont.)

Residual velocity amplitude due to an oscillatory velocity perturbation along the bottom

$$v_z(t) = v_0 \sin(2\pi(t - t_0)\nu)$$

with an amplitude of $v_0 = 50$ m/s and a frequency of $\nu_0 = 20$ mHz from $t = 1200$ s to $t = 1450$ s. Note the fast magnetic wave that gets refracted.

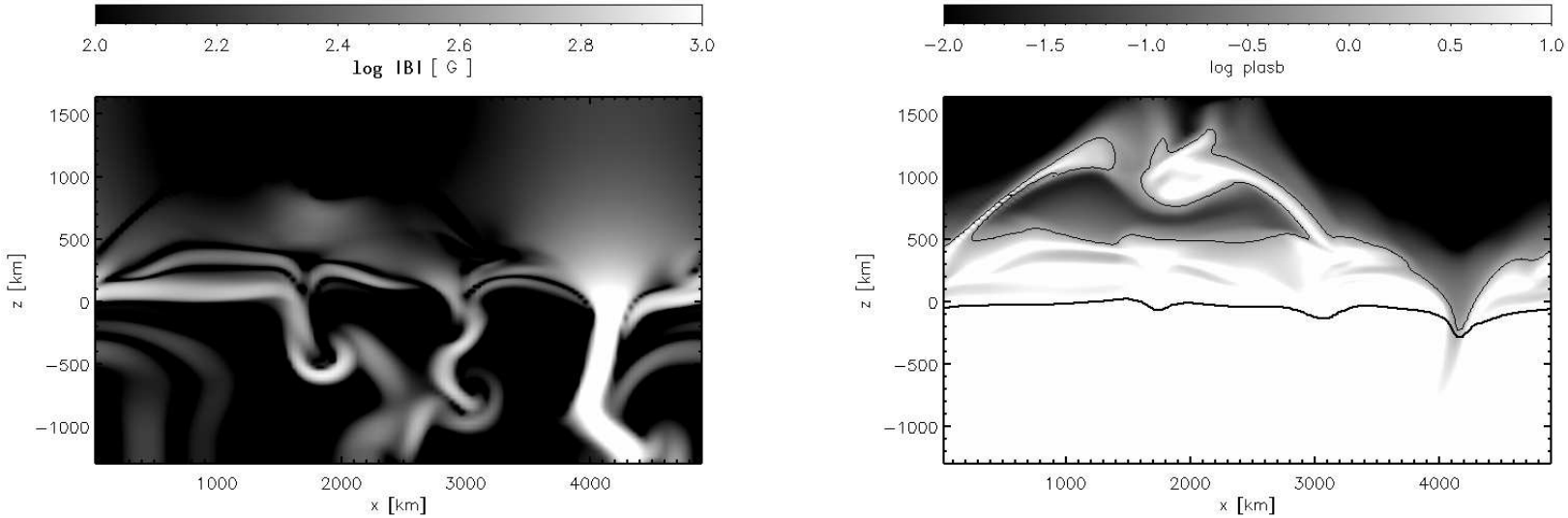

Left: Logarithmic magnetic field strength 1368 s after starting with an initial homogeneous vertical field of 100 G. *Right:* Logarithm of thermal to magnetic energy density (plasma-β) together with the conour of $\beta = 1$.

 Wave travel time vs. canopy height.

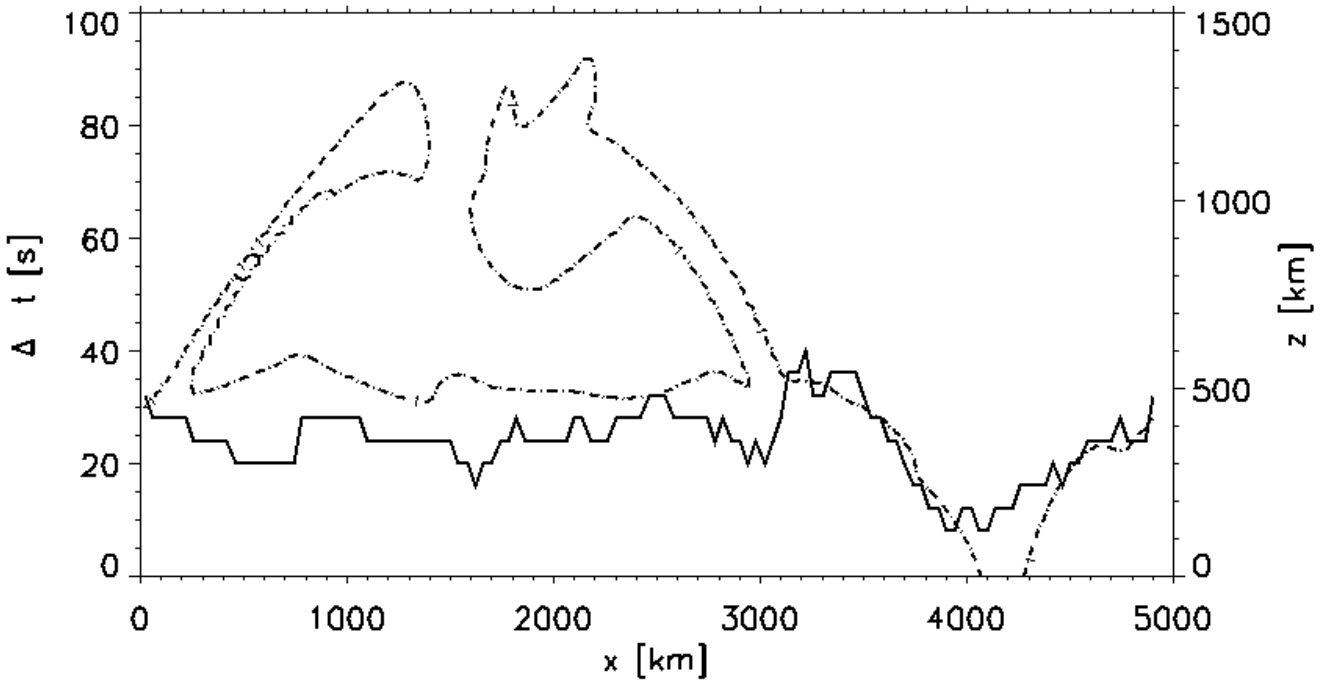

Wave travel time across the layer from $z = 200$ km to $z = 420$ km as a function of horizontal distance (thick solid curve). Superposed is the contour of $\beta = 1$ (magnetic and thermal equipartition), for which the height is indicated in the right hand side ordinate (dash-dotted curve). Note that the travel time markedly decreases where the low β region intrudes this layer. From *Steiner, Vigeesh, Krieger et al. 2007*

Coupling waves–magnetic field (cont.)

Finsterle et al. 2004, ApJ 613, L185 suggest to determine the three-dimensional topography of the $\beta = 1$-surface by measuring the travel time of high frequency waves between lines formed below and above this surface. They use a MOTH-MDI combined data set of 17.8 h duration

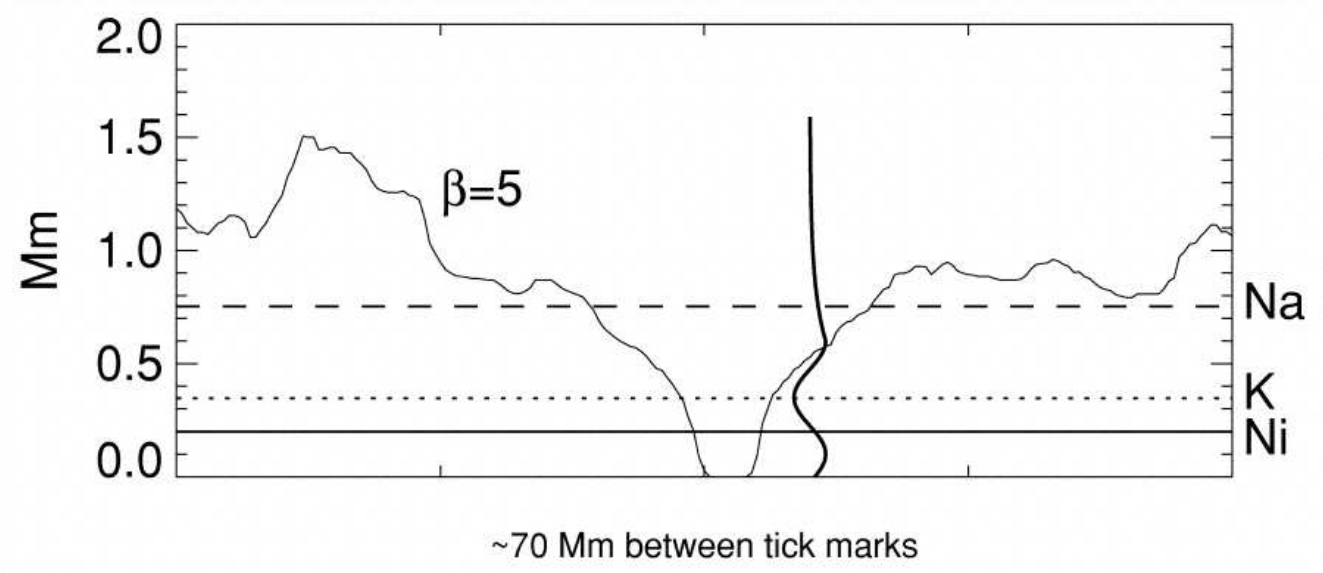

Helioseismic mapping of the magnetic canopy in the solar chromosphere

Coupling waves–magnetic field (cont.)

Maps of travel time for 7 mHz waves between the formation layers of (**a**) Ni and Na, (**b**) K and Na, and (**c**) Ni and K. (**d**) the contemporaneous MDI magnetogram. $\beta \approx 1$ contours at 200 km (white), 420 km (black-white), and 800 km (black) above $\tau_c = 1$.

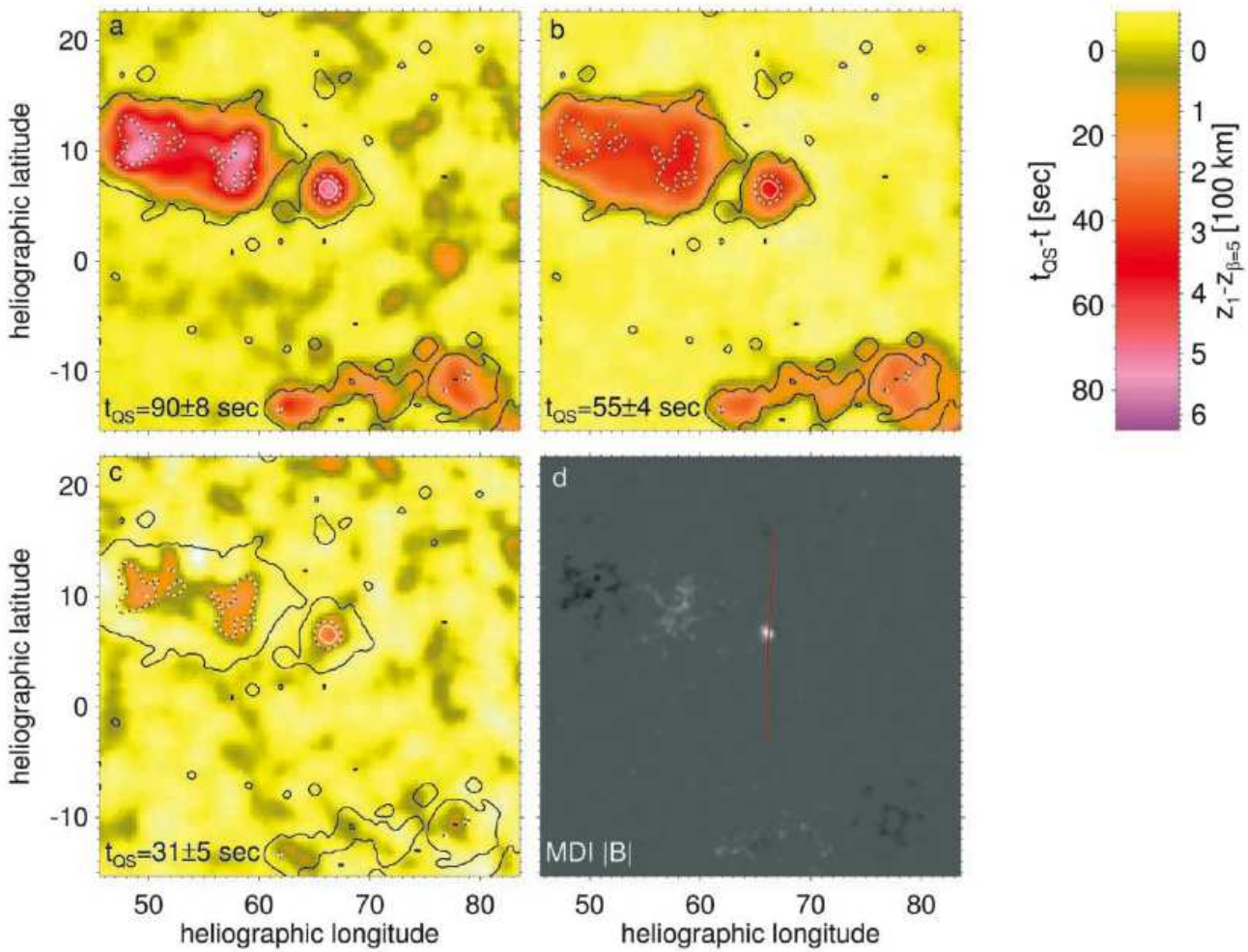

From *Finsterle et al. 2004, ApJ 613, L185*

Coupling waves–magnetic field (cont.)

Waves in the magnetized solar atmosphere

- Thomas, J.H.: 1982, ApJ 262, 760-767
- Zhugzhda & Dzhalilov: 1982, A&A 112, 16-23
- Zhugzhda & Dzhalilov: 1984, A&A 132, 45-51; A&A 132, 52-57; A&A 133, 333-340
- Shibata, K: 1983, PASJ 35, 263-284
- Rosenthal, Bogdan, Carlsson et al.: 2002, ApJ 564, 508-524
- Bogdan, Carlsson, Hansteen et al.: 2003, ApJ 599, 626-660
- Cally, P.S.: 2006, Phil. Trans. R. Soc. A: 2006, 364, 333-349
- Cally, P.S.: 2007, Astron. Notes/AN 328, 286-291
- Khomenko & Collados: 2006: ApJ 653, 739-755
- Khomenko, Collados & Felipe: 2008, 589-611
- Khomenko et al.: 2008, ApJ 676, L85-L88

Coupling waves–magnetic field (cont.)

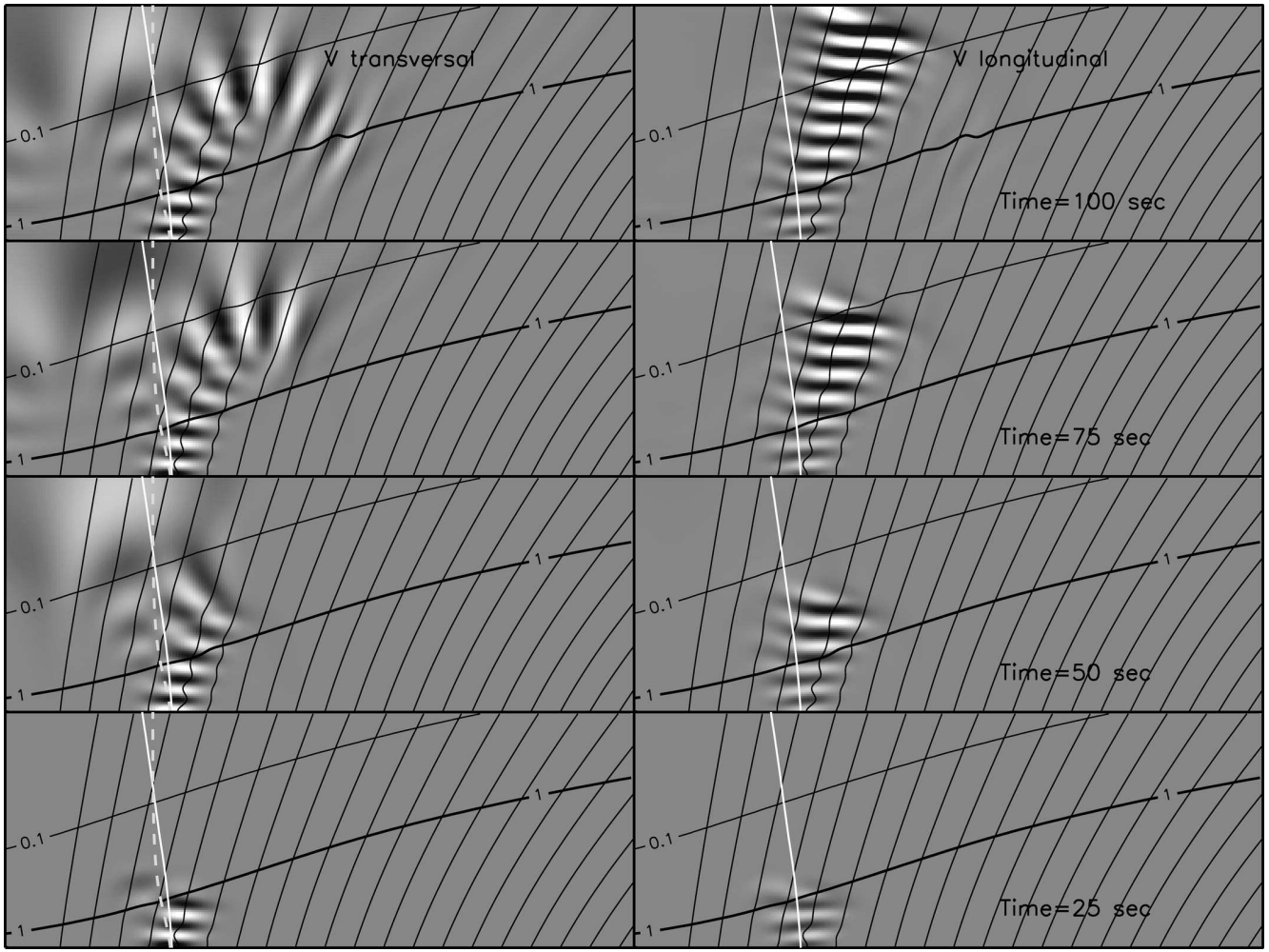

From *Khomenko & Collados, 2006, ApJ 653, 739*

Coupling waves–magnetic field (cont.)

Paul Cally (2007, Astron. Nachr./AN 328, 286–291) developed a modified ray theory. He studies a seismic wave with wave vector **k** approaching a magnetic region in a stratified medium from below.

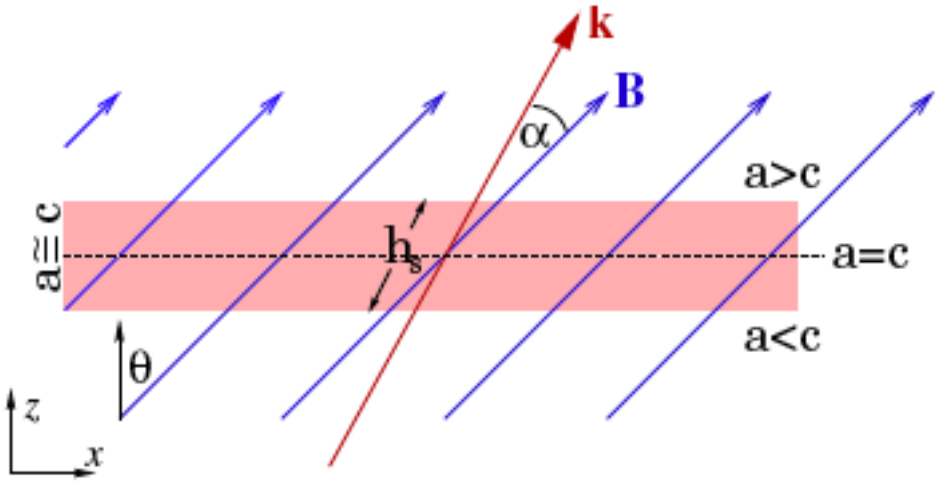

$$T = \exp\left[-\pi k h_s \sin^2 \alpha \right]_{a=c}$$

Coupling waves–magnetic field (cont.)

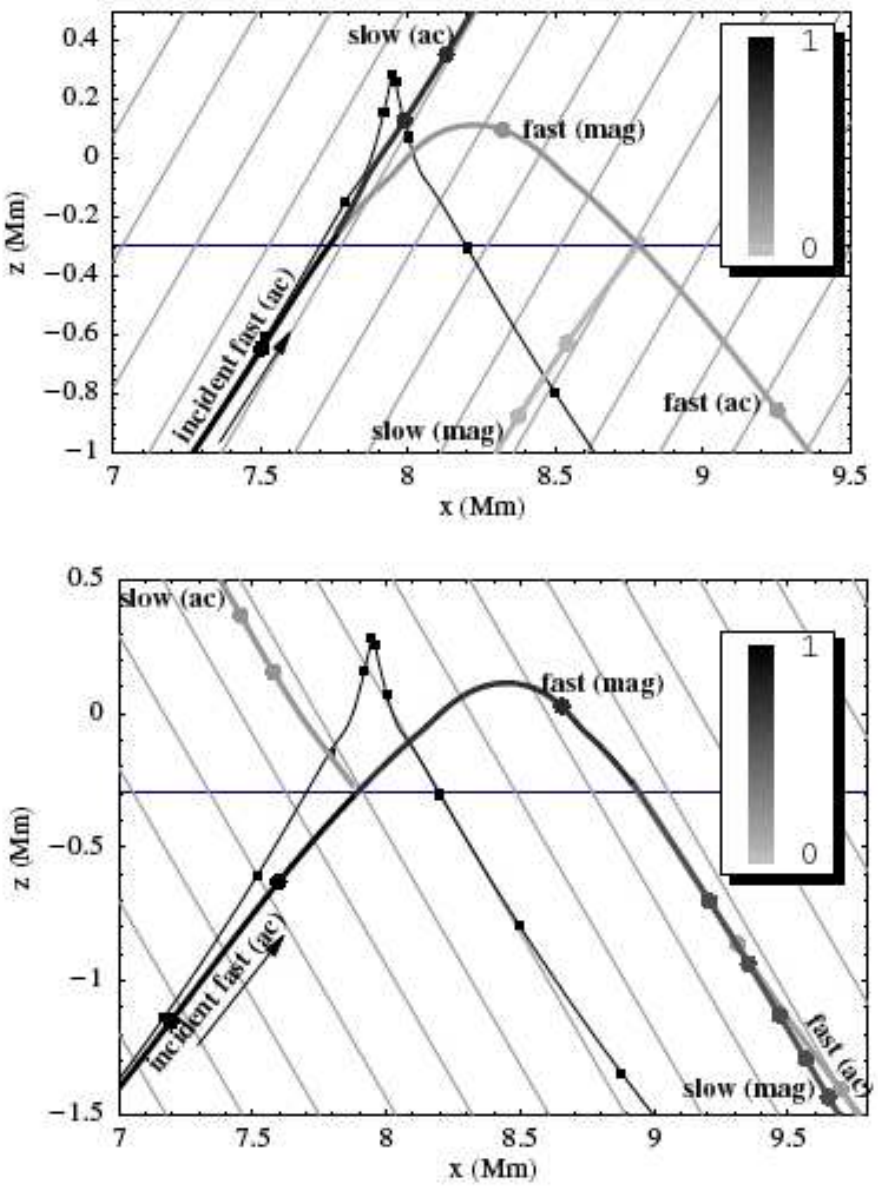

2 kG uniform magnetic field inclined at $\pm 30^\circ$ to the vertical. The incoming 5 mHz rays have lower turning points at $z = -5$ Mm. The horizontal grey line indicates where the sound and Alfvén speeds coincide. The fractional energy remaining in each resulting ray is indicated in grey scales. The dots on the ray paths indicate 1 min group travel time intervals. The thin black curve represents the acoustic ray that would be there in the absence of magnetic field. From *Cally (2007) AN 328, 286*

Movie top panel

Movie bottom panel

Coupling waves–magnetic field (cont.)

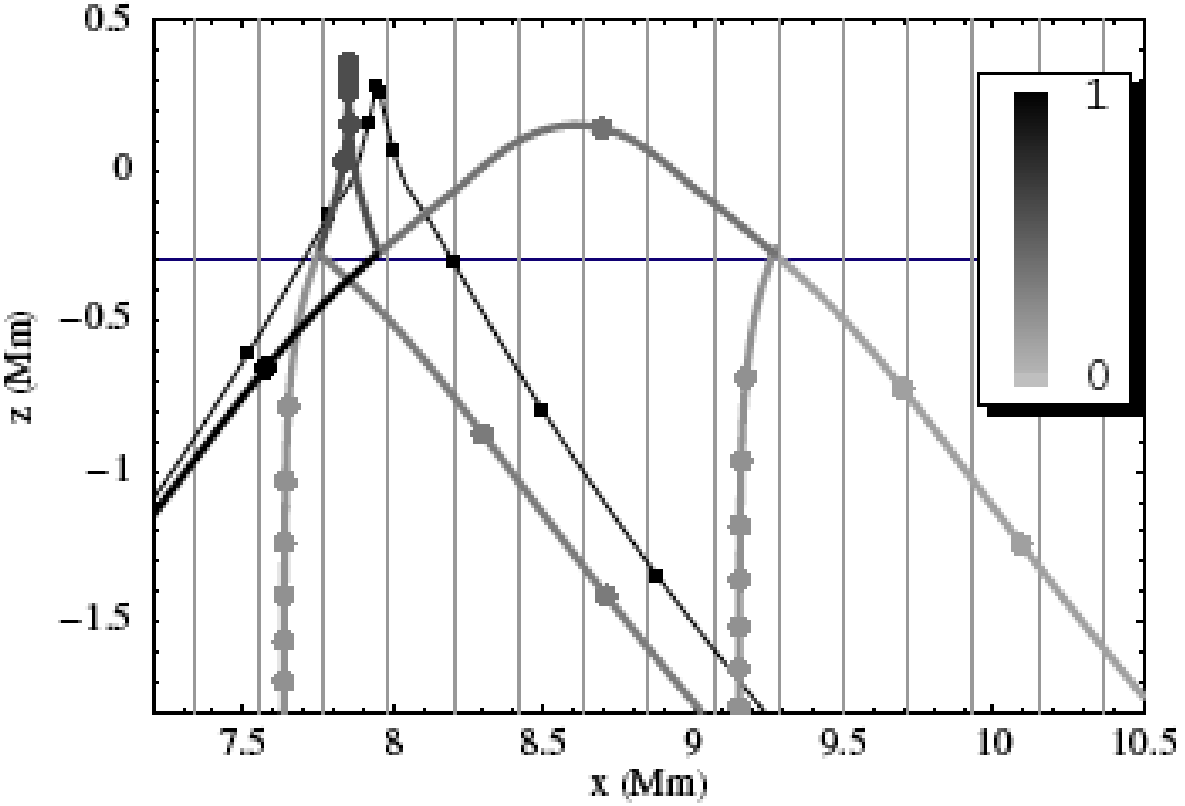

2 kG uniform vertical magnetic field. Here, the 5 mHz frequency is not sufficient to overcome the atmospheric acoustic cutoff (5.2 mHz), and the upgoing slow ray reflects back downward. From *Cally (2007) AN 328, 286*

Coupling waves–magnetic field (cont.)

Transversal, impulsive excitation at the footpoint of a magnetic flux sheet.

$v_x = v_0 \sin(2\pi t/P)$, $P = 24$ s, $v_0 = 750$ ms^{-1}

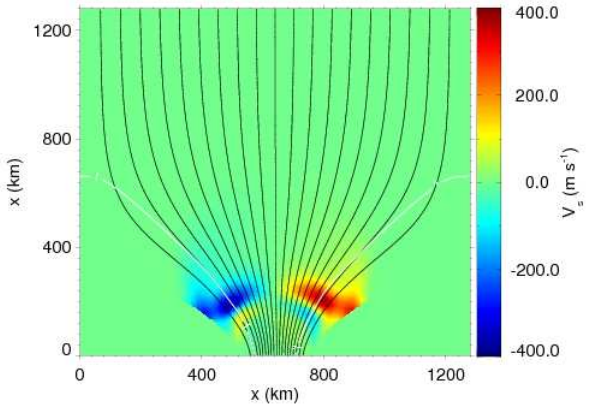

$v_{\parallel}$ after 40 s

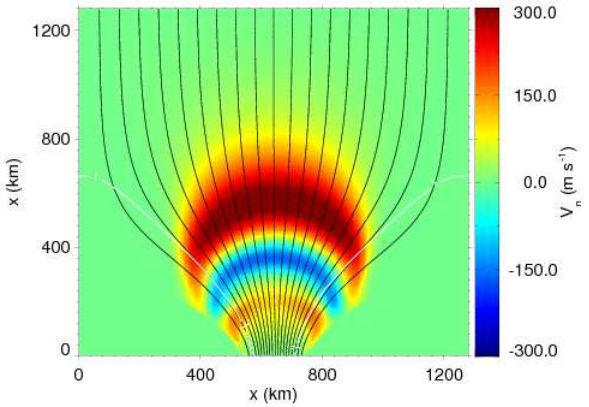

$v_{\perp}$ after 40 s

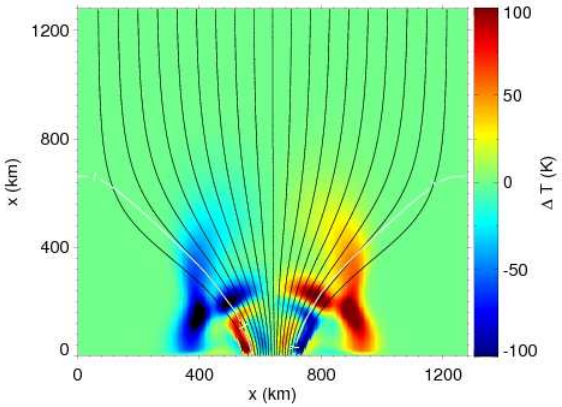

δT after 40 s

Vigeesh, Hasan, & Steiner in prep.

Coupling waves–magnetic field (cont.)

Energy flux as a function of time on a field line that encloses a fractional flux of 50%.

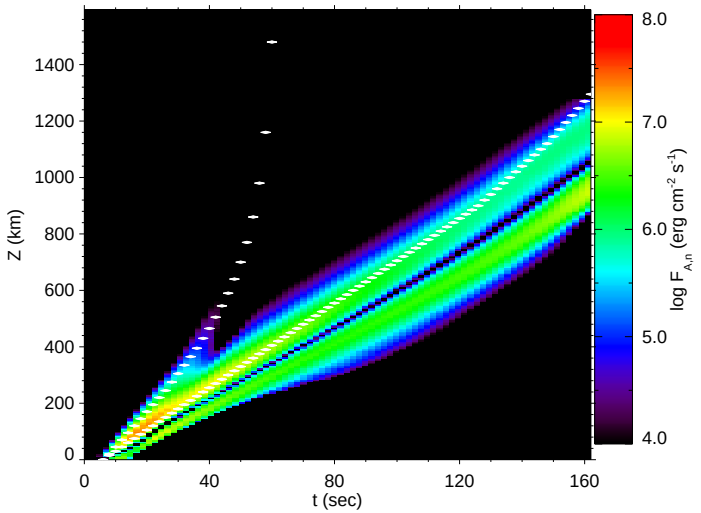

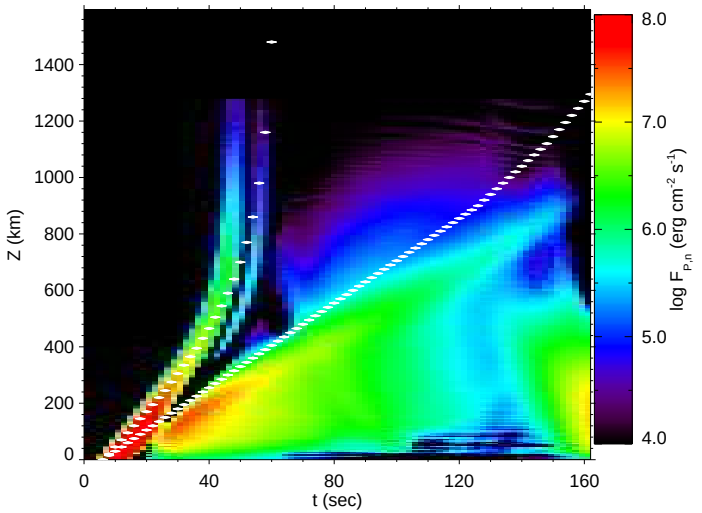

Acoustic flux $\Delta p\,\mathbf{v}$

Poynting flux $[(\mathbf{B}_0 \cdot \Delta\mathbf{B})\mathbf{v} - (\mathbf{v}\Delta\mathbf{B})\mathbf{B}_0]/\mu$

Initial Excitation	$F_{A,z}$ (10^6 erg cm^{-2} s^{-1}) z=1 000 km	$F_{P,z}$ (10^6 erg cm^{-2} s^{-1}) z=1 000 km
0.75 km s^{-1}, 24s	1.33	0.14
0.75 km s^{-1}, 120s	4.02	0.07
0.75 km s^{-1}, 240s	3.30	0.02
1.50 km s^{-1}, 24s	3.34	0.57
3.00 km s^{-1}, 24s	6.22	2.31

Coupling waves–magnetic field (cont.)

Reduction of the cutoff frequency by radiative damping.

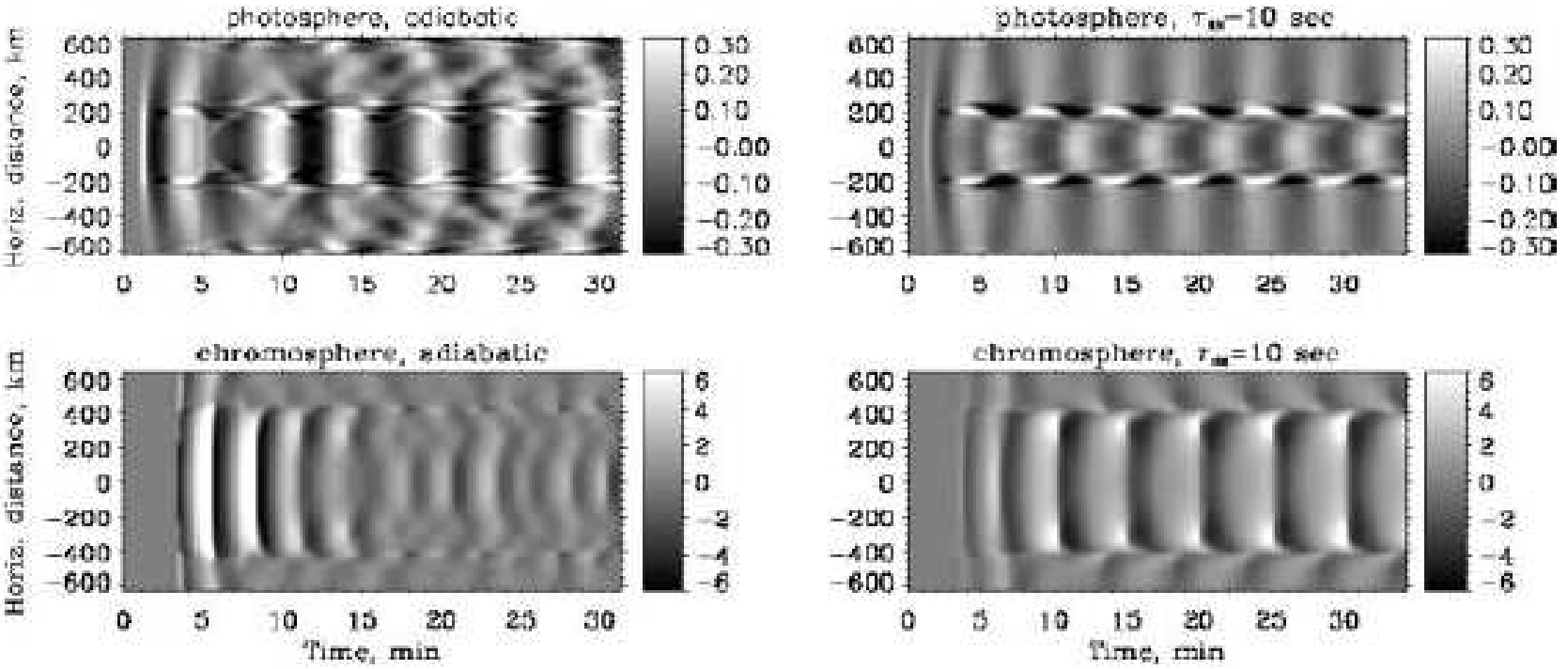

Propagation from a 3 mHz wave from the photosphere (top panels) to the chromosphere (bottom panels) in the adiabatic case (left) and with a radiative relaxation time of 10 s (right). In the latter case the wave passes unaltered into the chromosphere.

From *Khomenko et al., ApJ 676, L85 (2008)*

Coupling waves–magnetic field (cont.)

The formation of Ca II H_{2v} and K_{2v} bright points was shown to be the consequence of shock formation in the chromosphere. *Carlsson & Stein 1997, ApJ 481, 500-514*

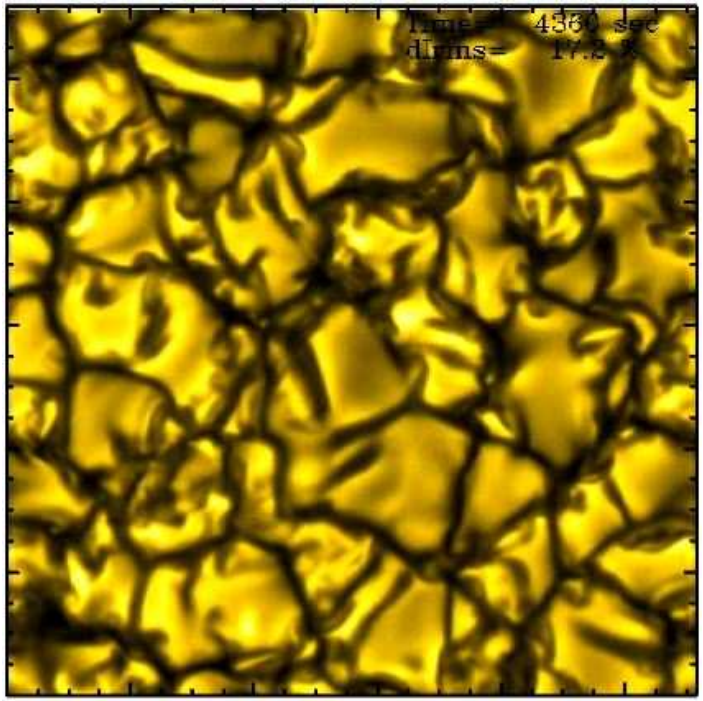

Simulation of solar granulation with *CO^{5}BOLD*. 12×12 Mm.

Courtesy, M. Steffen AIP

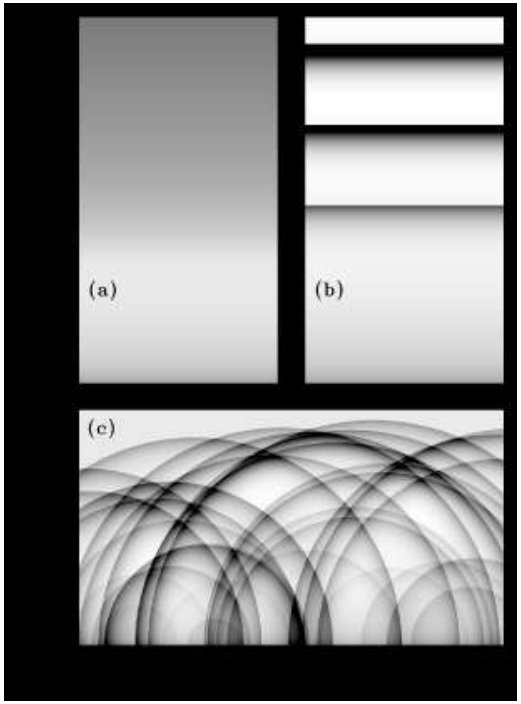

From S. Cranmer. Courtesy, W. Rammacher

2-D CO^{5}BOLD simulation including the chromosphere by S. Wedemeyer-Böhm

Coupling waves–magnetic field (cont.)

Correspondingly one sees a fast changing pattern of enhanced temperatures in the chromosphere, *the fluctosphere*, differently from the pattern of inverse granulation in the middle photosphere, and the granulation itself.

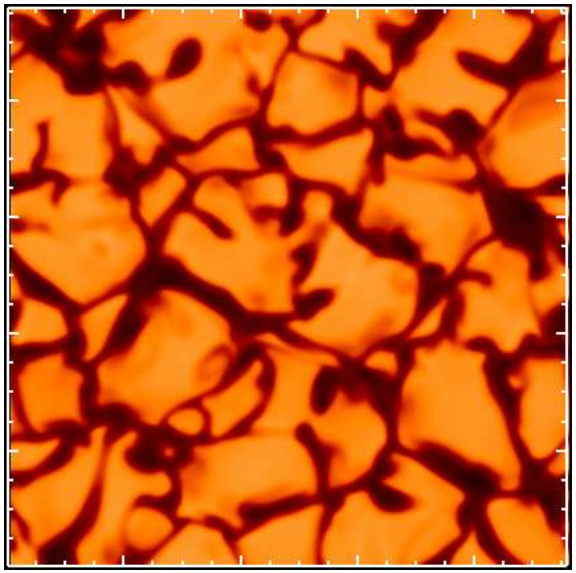

$T(z = -200\mathrm{km})$

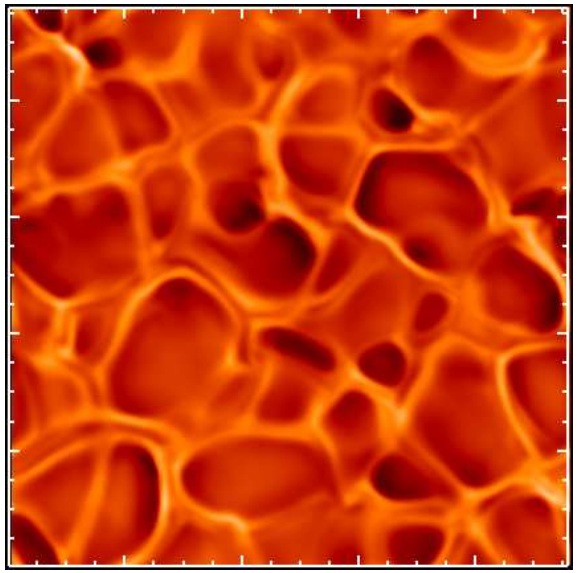

$T(z = +200\mathrm{km})$

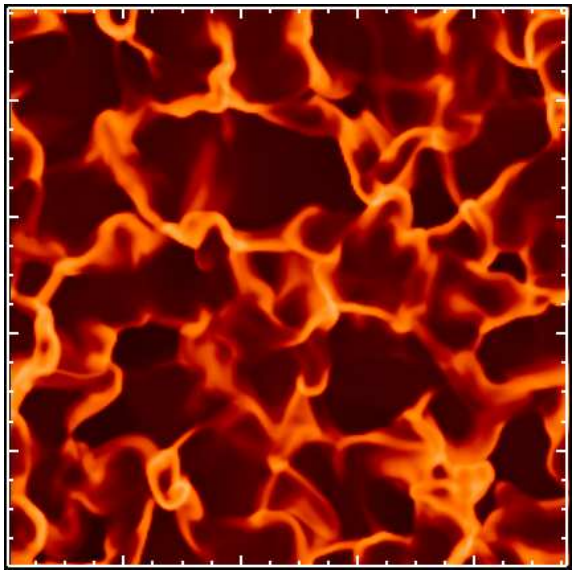

$T(z = +1000\mathrm{km})$

Coupling waves–magnetic field (cont.)

Filtergrams in the infrared line Ca II 854 nm

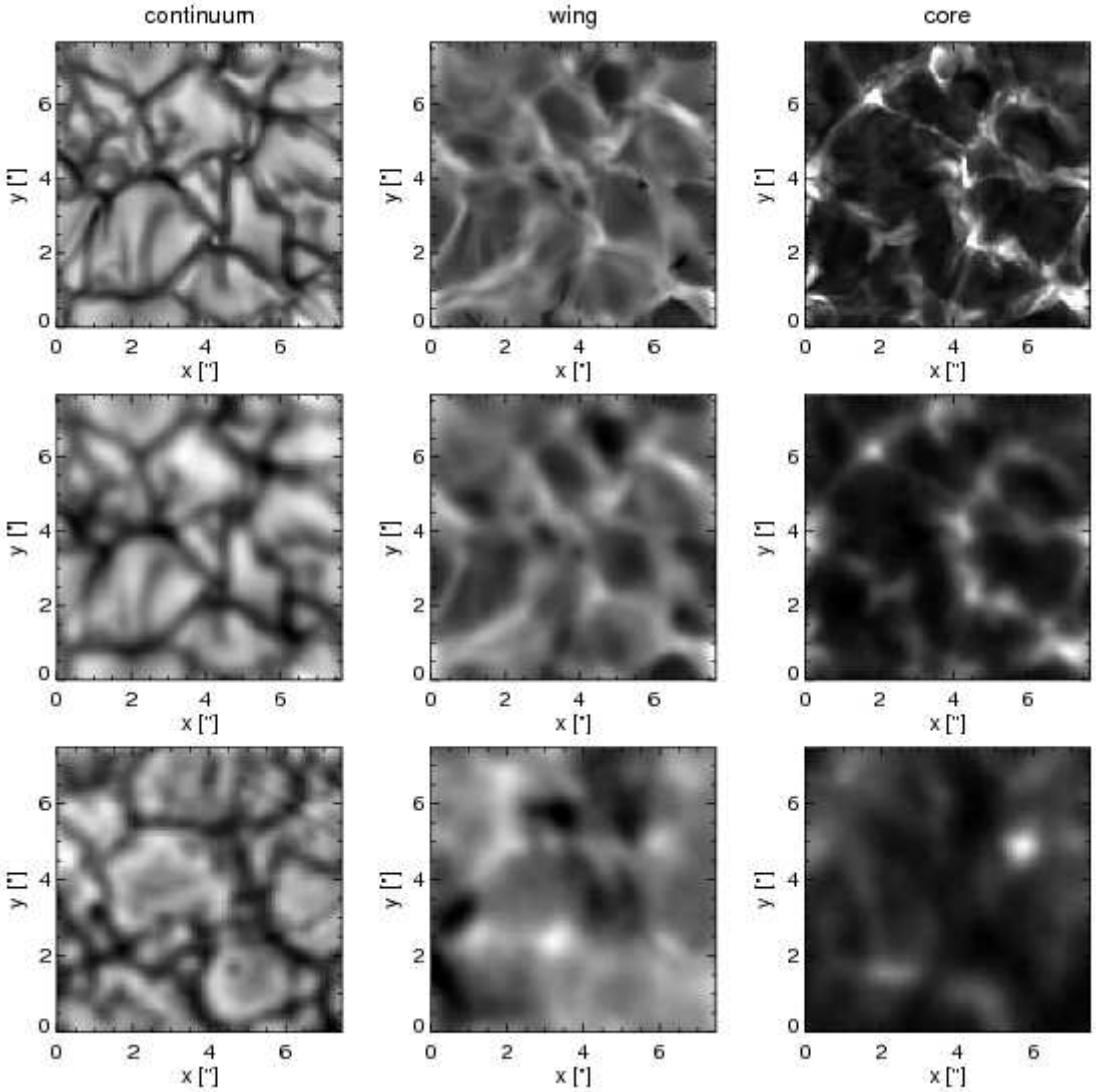

simulation

simulation + PSF

observation

Wöger et al. 2006

observed in 0.3 Å filtergrams centred at the Ca II K_{2v} peak a short-lived pattern with a typical spatial scale of 1.95” and a mean evolution time scale of 53 s.

Courtesy, S. Wedemeyer-Böhm

Coupling waves–magnetic field (cont.)

Intensity image at $\lambda = 1$ mm of the "fluctosphere" at different spatial resolutions:

a) 0.06" (size of computational grid cells), **b**) 0.3", **c**) 0.6", **d**) 0.9".

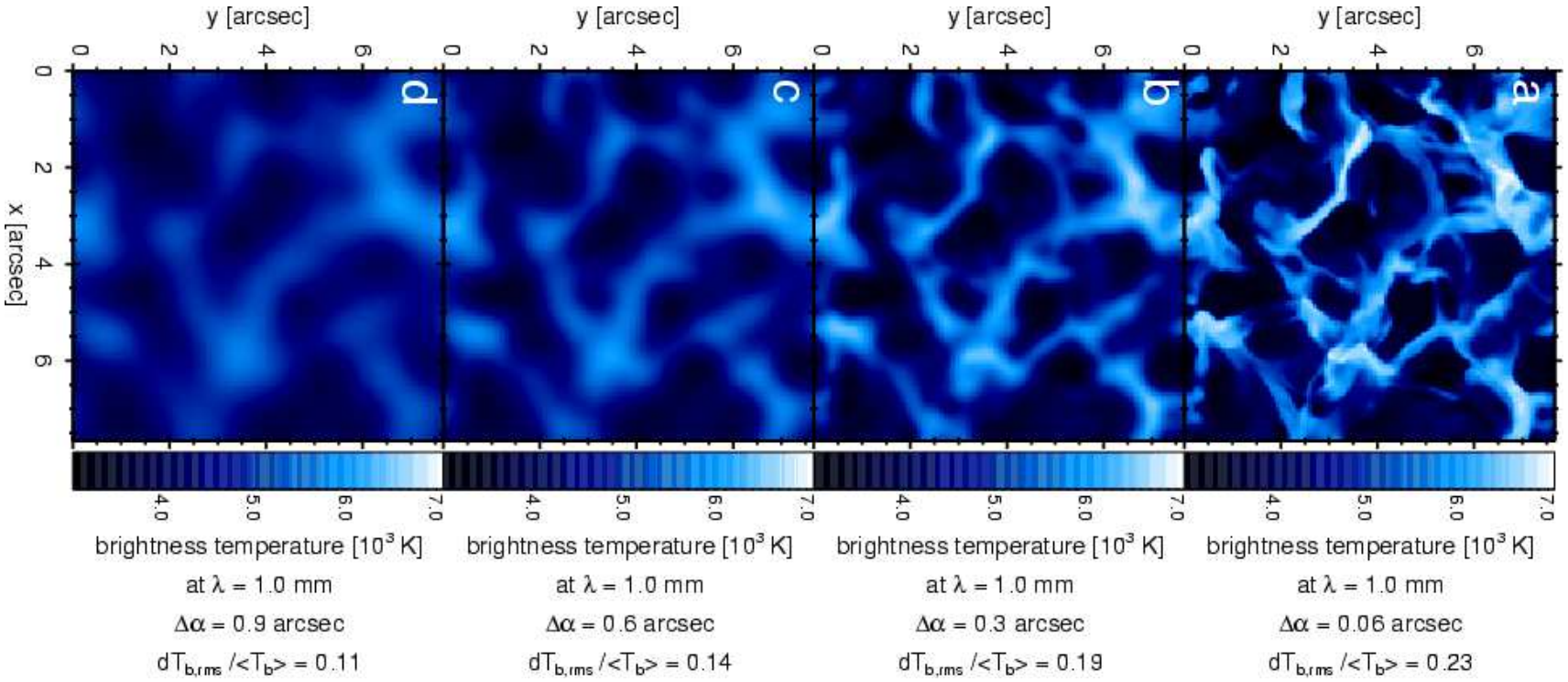

From *Wedemeyer-Böhm et al., A&A 471, 977 (2007)*

Coupling waves–magnetic field (cont.)

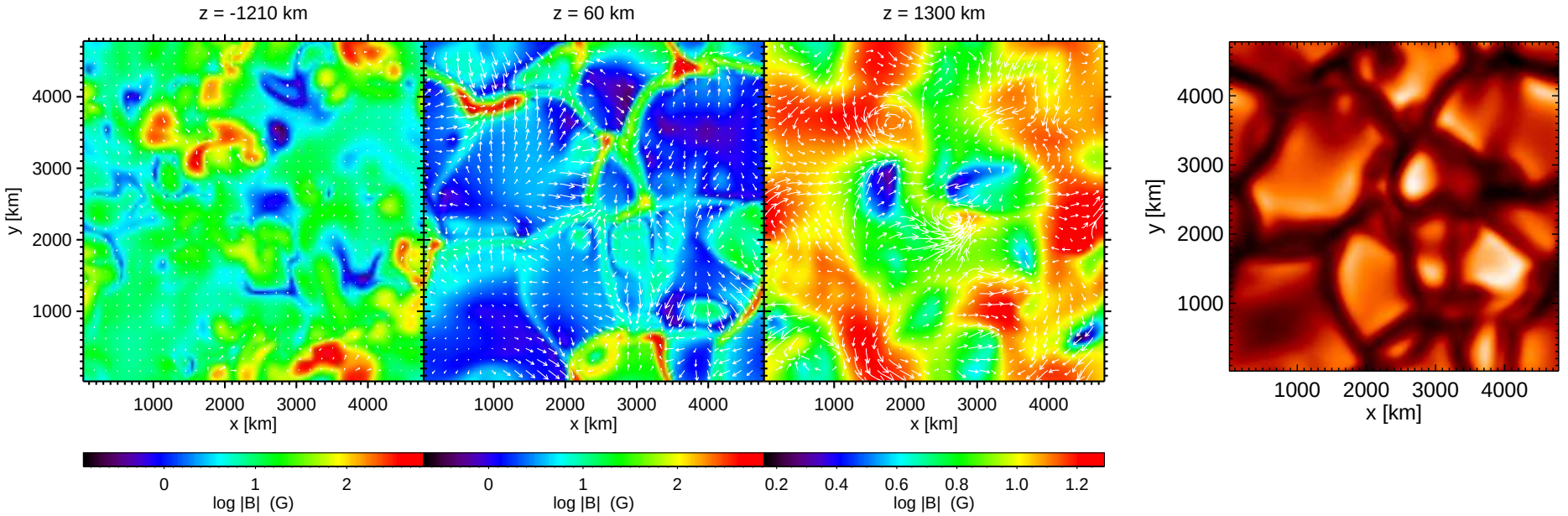

Horizontal sections through 3-D computational domain. Color coding displays $\log|B|$ with individual scaling for each panel. **Left:** Bottom layer at a depth of 1210 km. **Middle:** Layer 60 km above optical depth $\tau_c = 1$. **Right:** Top, chromospheric layer in a height of 1300 km. White arrows indicate the horizontal *velocity* on a common scaling. Longest arrows in the panels from left to right correspond to 4.5, 8.8, and 25.2 km/s, respectively. **Rightmost:** Emergent *intensity*.

Coupling waves–magnetic field (cont.)

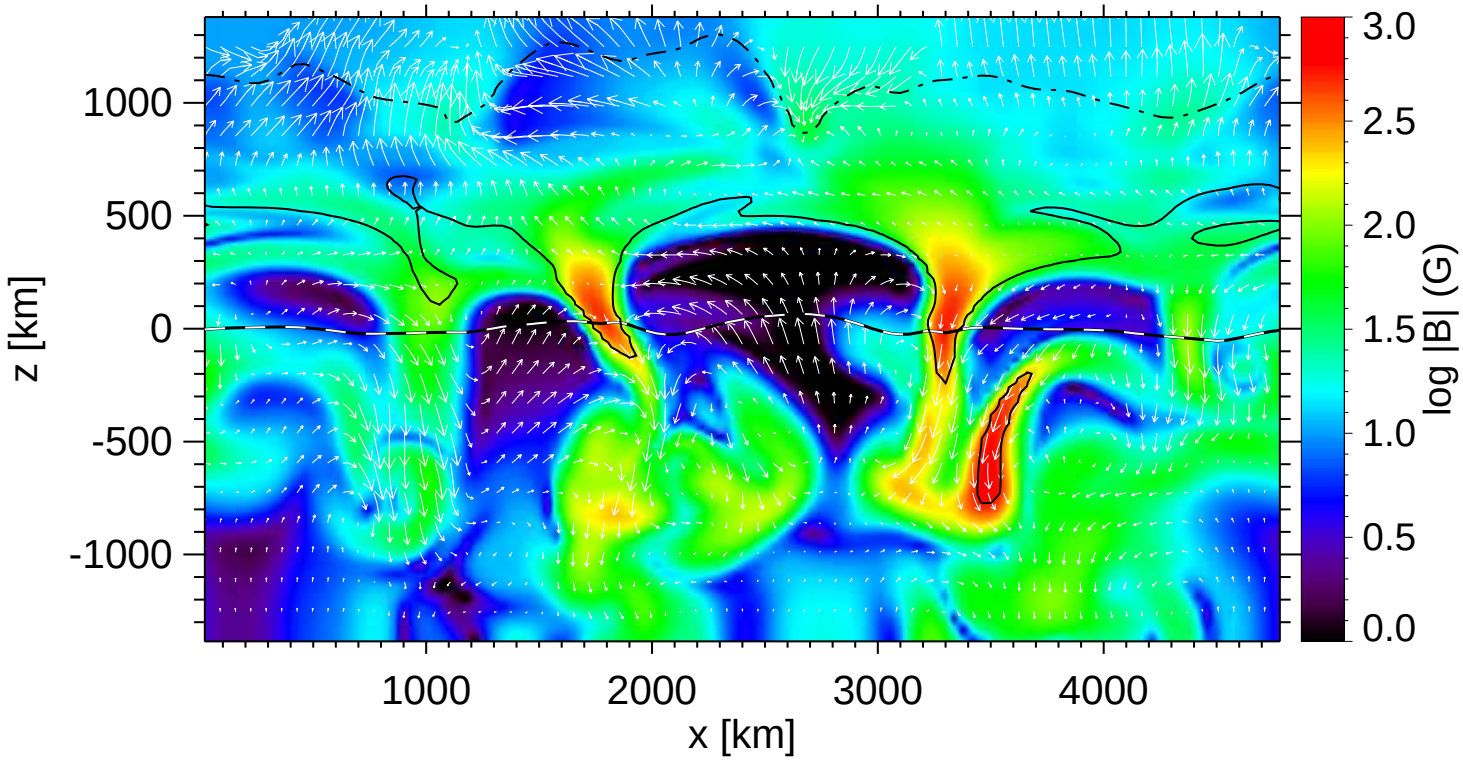

Snapshot of a vertical section showing $\log|B|$ (color coded) and *velocity vectors* projected on the vertical plane (white arrows). The b/w dashed curve shows optical depth unity and the dot-dashed and solid black contours $\beta = 1$ and 100, respectively. movie with $\beta = 1$ surface

Schaffenberger, Wedemeyer-Böhm, Steiner & Freytag, 2005, in *Chromospheric and Coronal Magnetic Fields*, Innes, Lagg, Solanki, & Danesy (eds.), ESA Publication SP-596

Coupling waves–magnetic field (cont.)

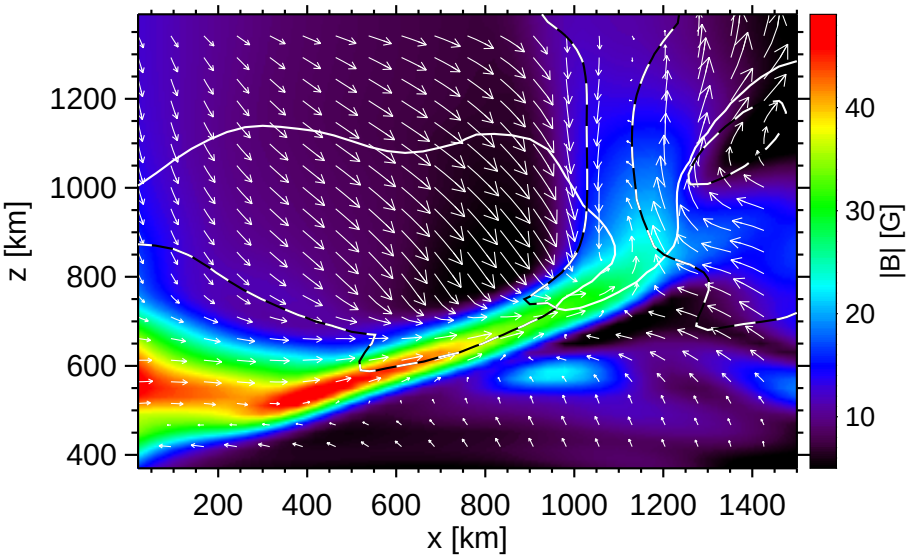

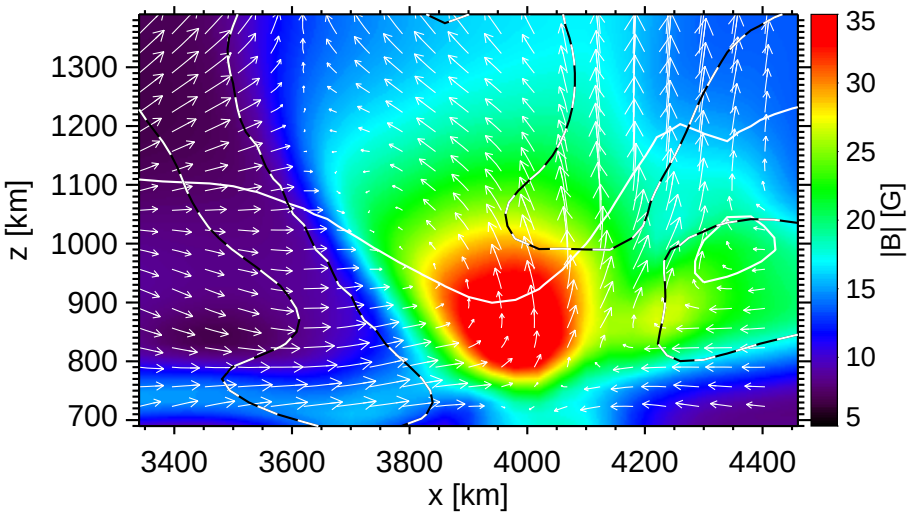

Two instances of shock induced magnetic field compression. Absolute magnetic flux density (colors) with velocity field (arrows), $\mathrm{Mach} = 1$-contour (dashed) and $\beta = 1$-contour (white solid).

Coupling waves–magnetic field (cont.)

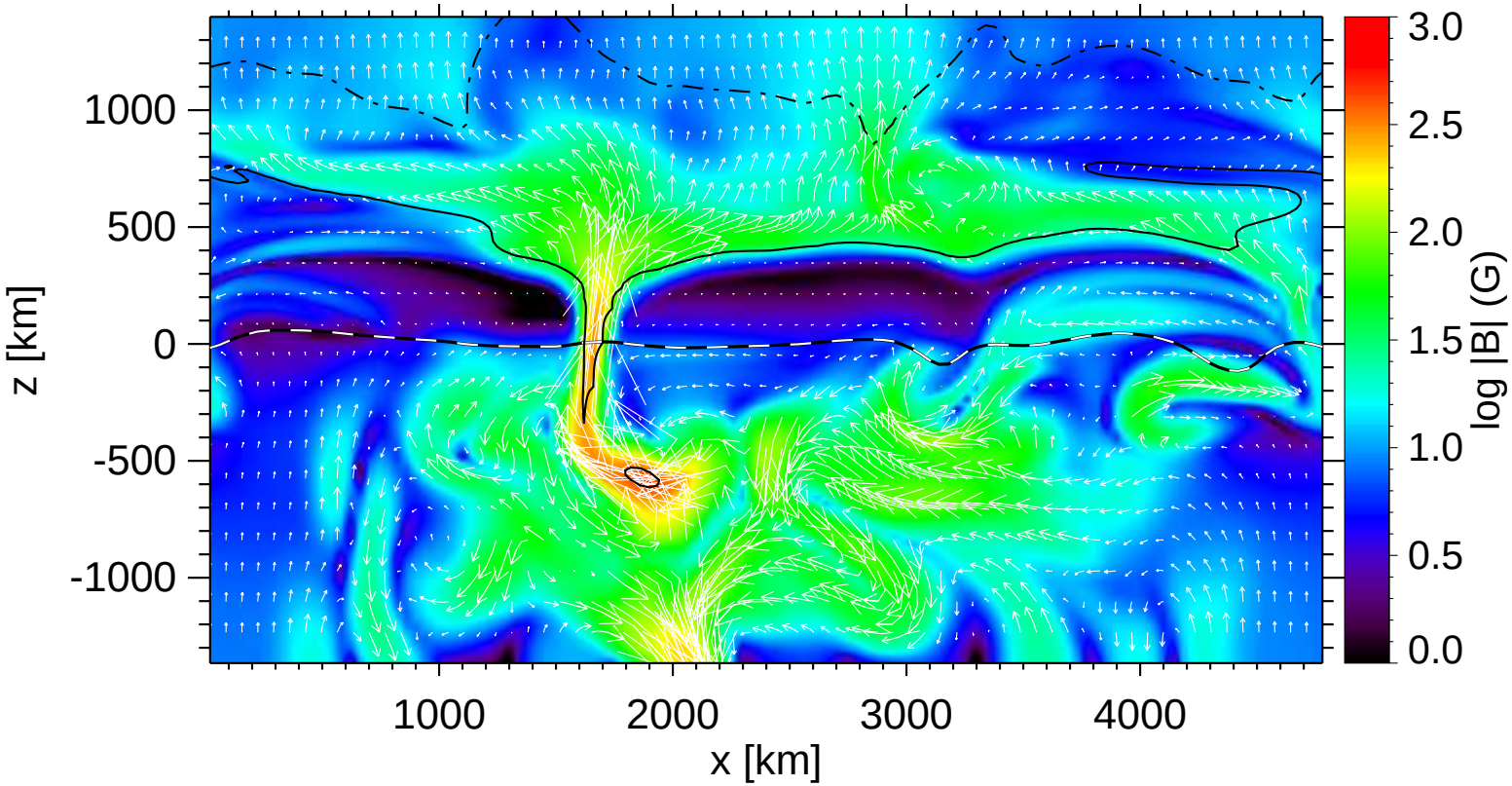

Snapshot of a vertical section showing $\log|B|$ (color coded) and $\mathbf{B}$ projected on the vertical plane (white arrows). The b/w dashed curve shows optical depth unity and the dot-dashed and solid black contours $\beta = 1$ and 100, respectively. Schaffenberger, Wedemeyer-Böhm, Steiner & Freytag, 2005, in *Chromospheric and Coronal Magnetic Fields*, ESA Publication SP-596

Coupling waves–magnetic field (cont.)

It was argued (Schrijver & Title, 2003) that weak flux concentration in the internetwork would destroy any large scale magnetic canopy field. However ....

Coupling waves–magnetic field (cont.)

It was argued (Schrijver & Title, 2003) that weak flux concentration in the internetwork would destroy any large scale magnetic canopy field. However ....

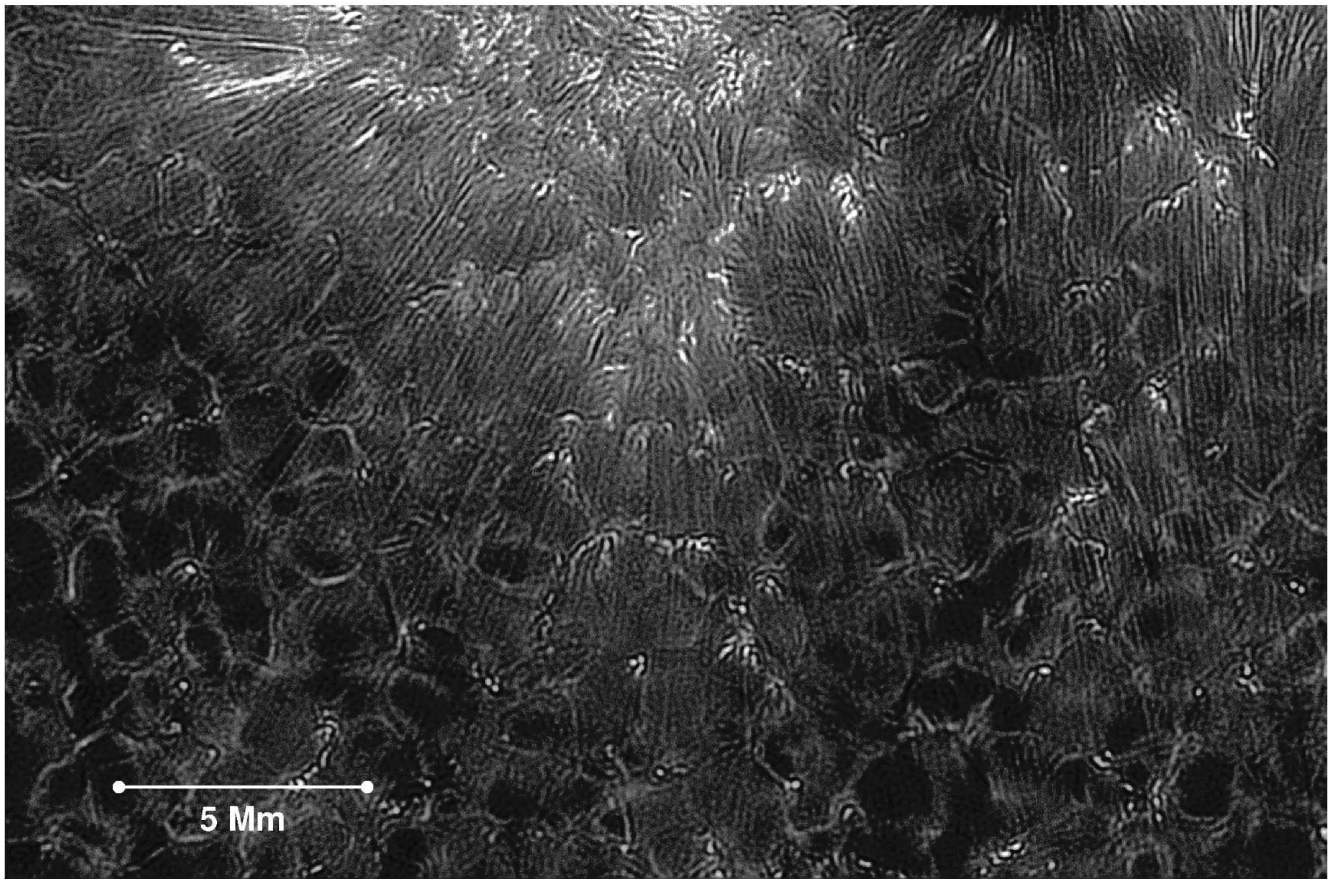

Narrow band (0.1Å) image (contrast enhanced) of a plage region observed in the line core of Ca K using the SST *Courtesy A. Pietarila*

Coupling waves–magnetic field (cont.)

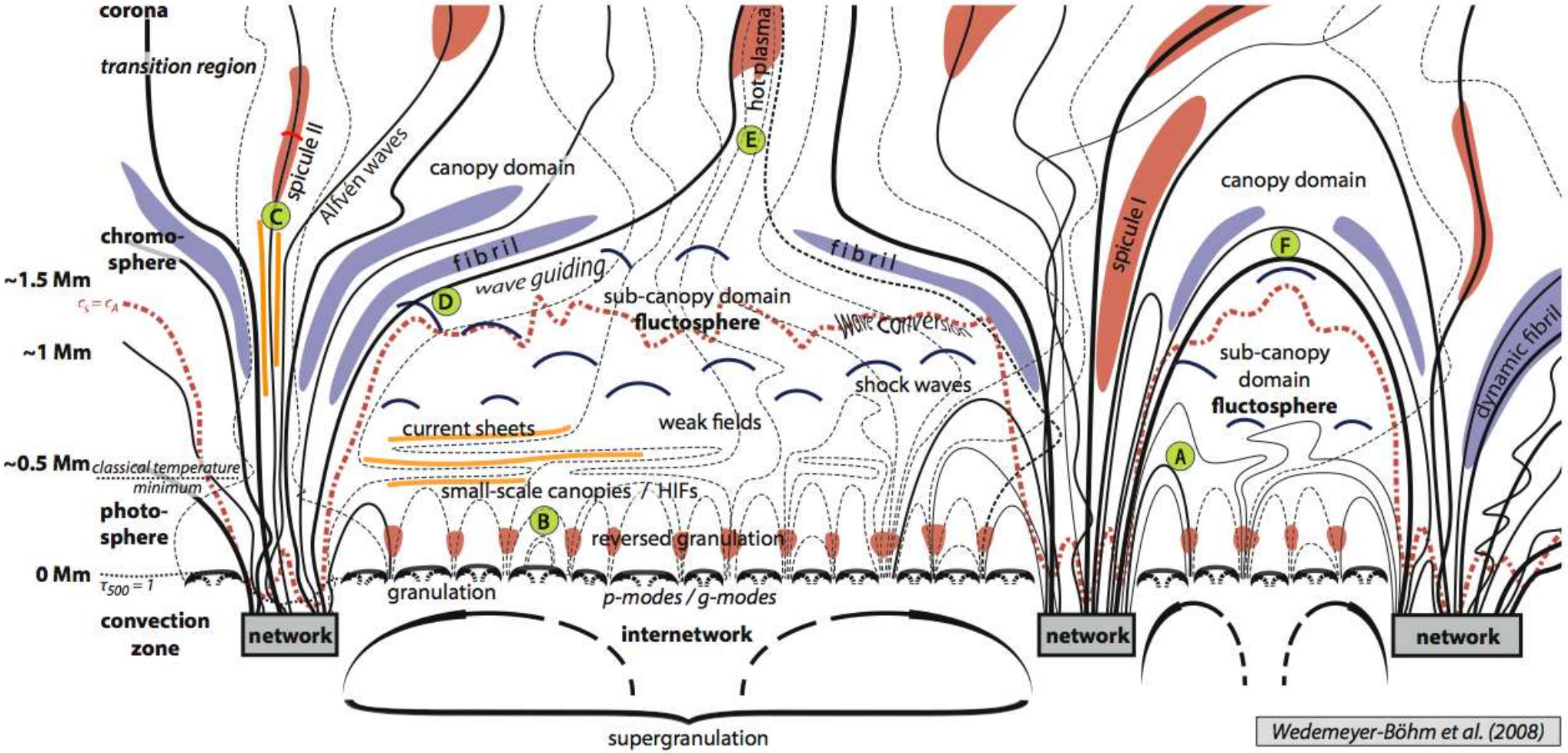

Schematic quiet Sun atmosphere. From *Wedemeyer-Böhm, Lagg, & Nordlund, ISSI review*

5. Coupling magnetic field–radiation

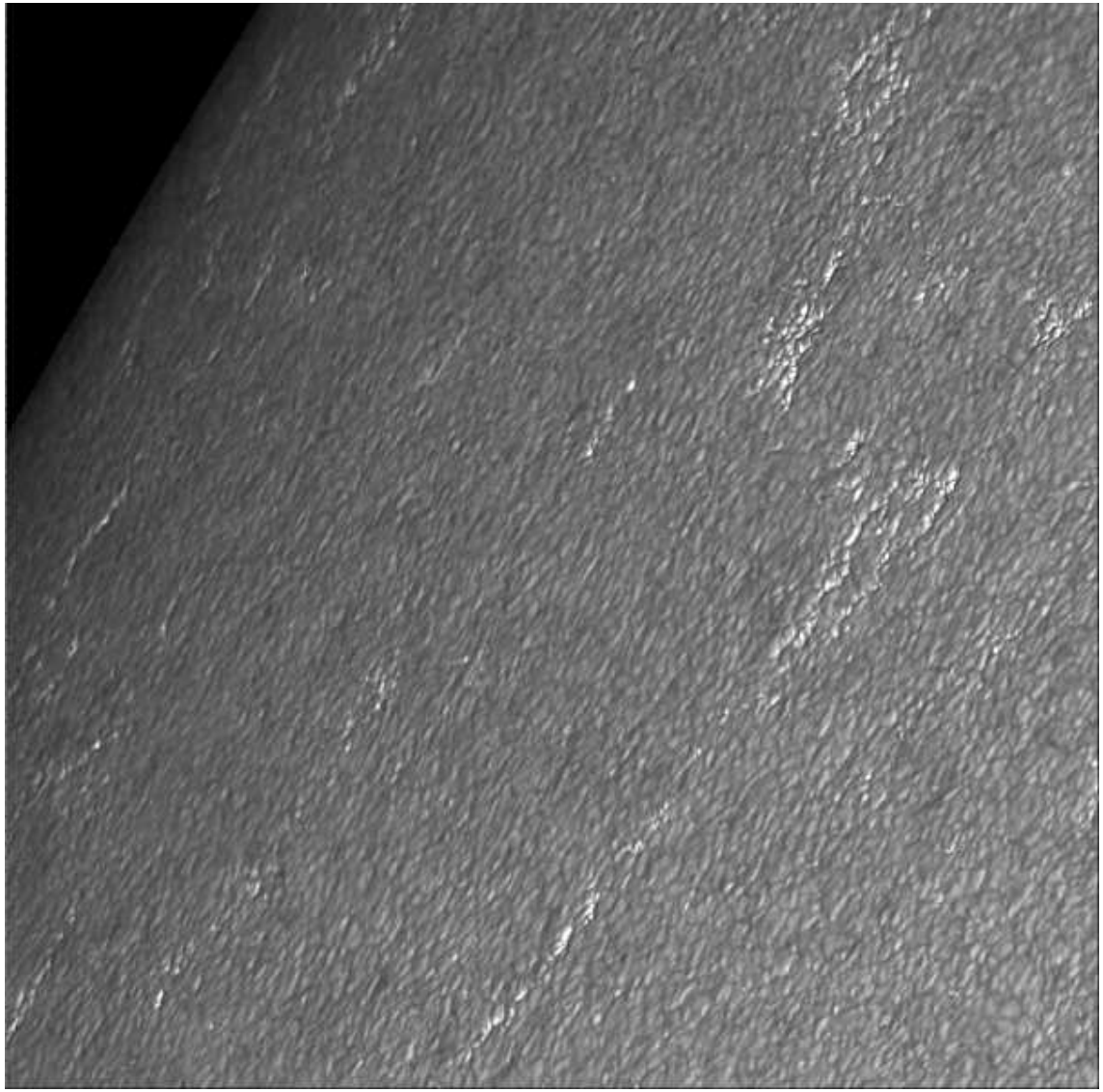

Speckle reconstructed image of facular region taken with the 1 m Swedish Solar Telescope in the continuum at 487.5 nm. Field of view approximately $80'' \times 80''$.

From Hirzberger & Wiehr (2005), A&A 438, 1059

There exists a long list of *center to limb* measurements of the *continuum contrast* of faculae. The measurements are contradictory because they are spatial resolution dependent and because of selection effects. There exists an equally long list of models most notable the *"hot wall" model* of Spruit (1976).

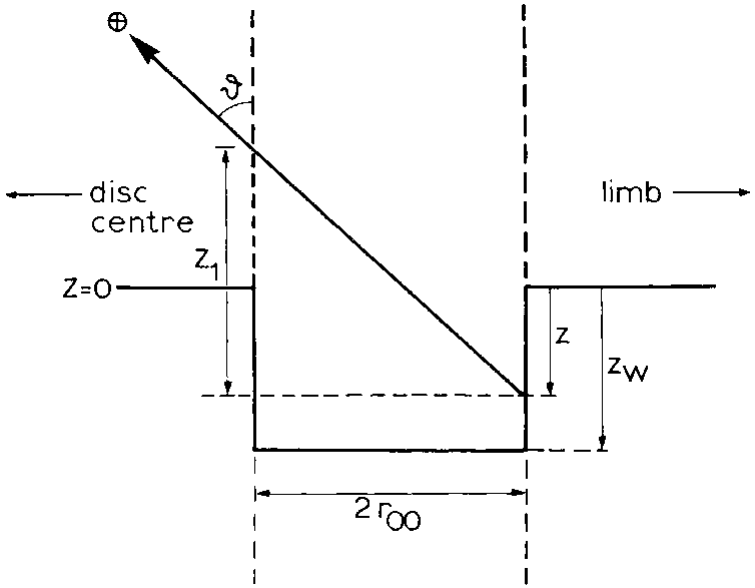

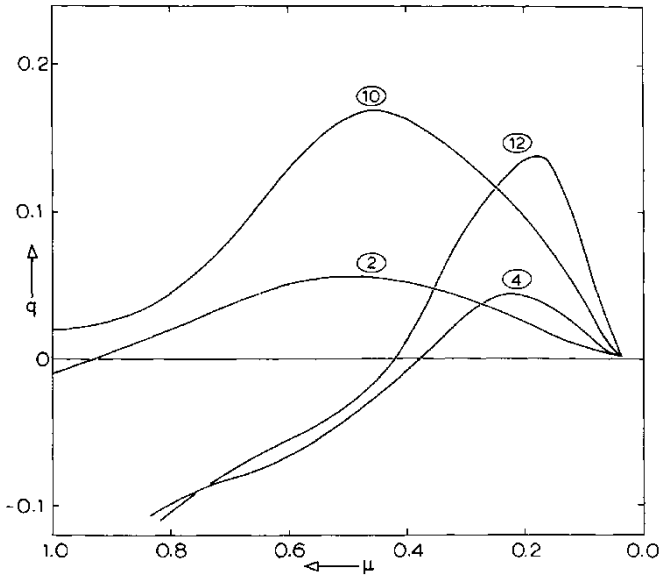

From Spruit (1976), Sol. Phys. 50, 269

Coupling magnetic field–radiation (cont.)

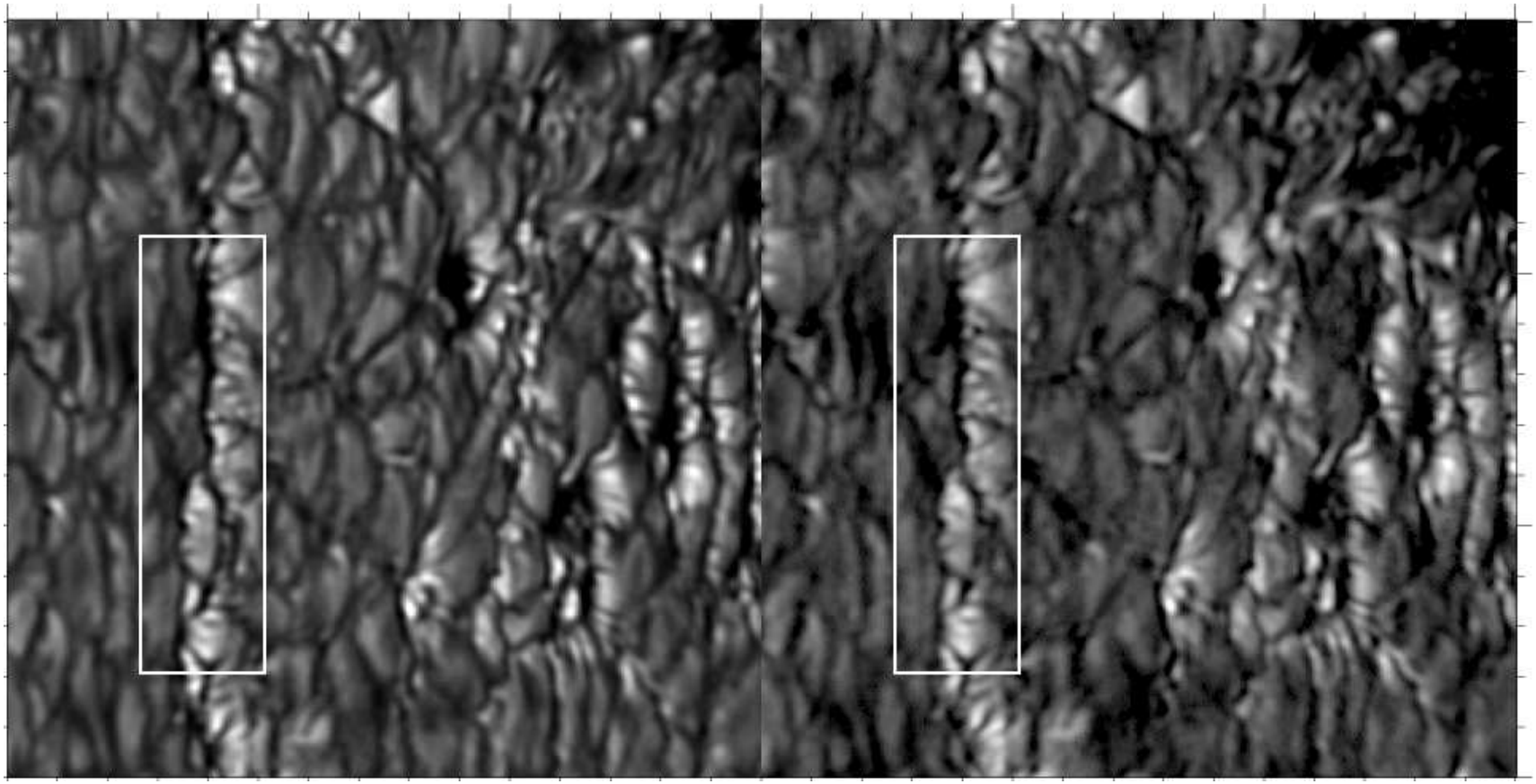

Faculae at $\theta = 61^\circ$ in the continuum at 587.5 nm (left) and in the G-band (right). Solar limb is right. Tickmarks indicate $1''$ distances. The facular brightening occurs on the disk-center side of granules limbward of a dark "facular lane".

From Hirzberger & Wiehr (2005), A&A 438, 1059

Coupling magnetic field–radiation (cont.)

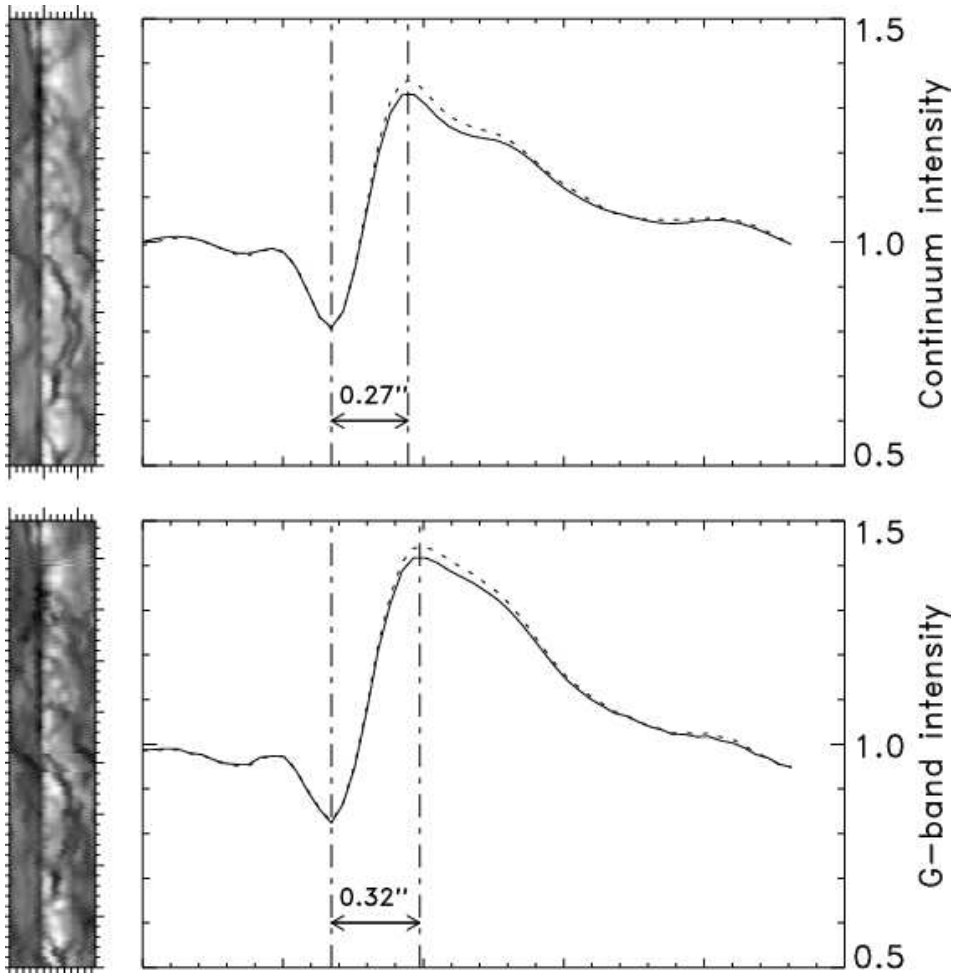

Mean spatial scan through faculae at $\theta = 61^\circ$ in the 587.5 nm continuum (top) and in the G-band (bottom). Note the flat limbward decrease and the centerward dark "facular lane".

From Hirzberger & Wiehr (2005), A&A 438, 1059

Coupling magnetic field–radiation (cont.)

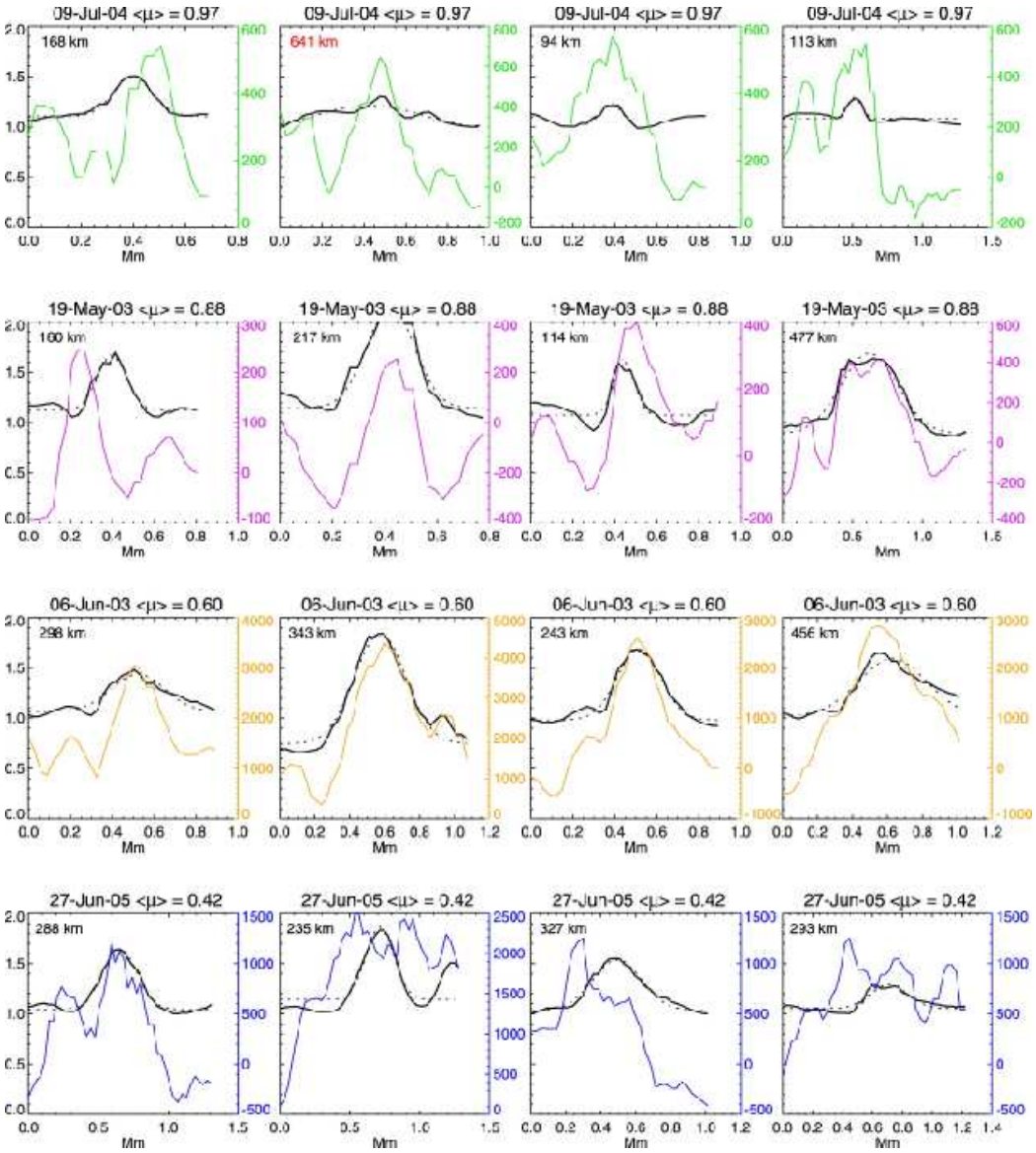

From *Berger et al. ApJ 661, 1272 (2007)* Solid black: G-band intensity profile solid colored: magnetogram profile.

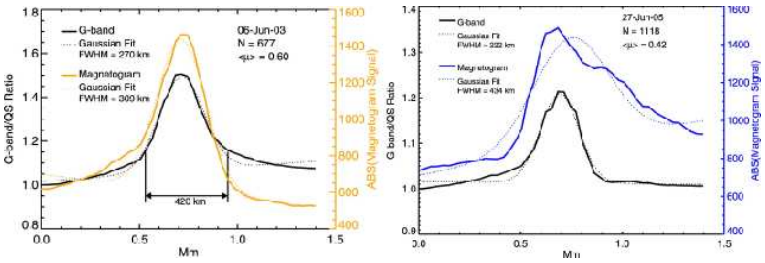

Coupling magnetic field–radiation (cont.)

- From a location at the solar surface and lateral to the flux sheet one “sees” a *more transparent sky* in the direction to the flux sheet compared to a direction under equal zenith angle but away from it.

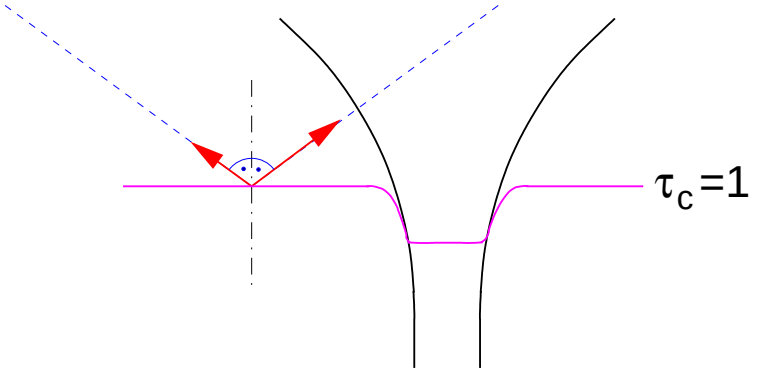

- Correspondingly, from a *wide area* surrounding the magnetic flux sheet or flux tube, radiation escapes more easily in the direction of the flux sheet/tube.

- A single flux sheet/tube impacts the radiative escape in a cross-sectional area (*“radiative cross section”*) that is much wider than the magnetic field concentration proper.

Chevalier, S. (1912), Ann. de l'Obs. de Zô-sè, 8, C1

"La granulation que l'on voit autour des taches plus éclatante que sur les autres parties est-ell la granulation des facules ou celle de *la photosphère vue à travers les facules* ?"

ten Bruggencate, P. (1939), Zeitschrift f. Astroph. 19, 59

.... Photosphärengranulen und *Fackelgranulen*. Sie unterscheiden sich nicht durch ihre mittlere Grösse, wohl aber durch den Kontrast gegenüber der Umgebung.

Coupling magnetic field–radiation (cont.)

From Steiner (2005) A&A 430, 691

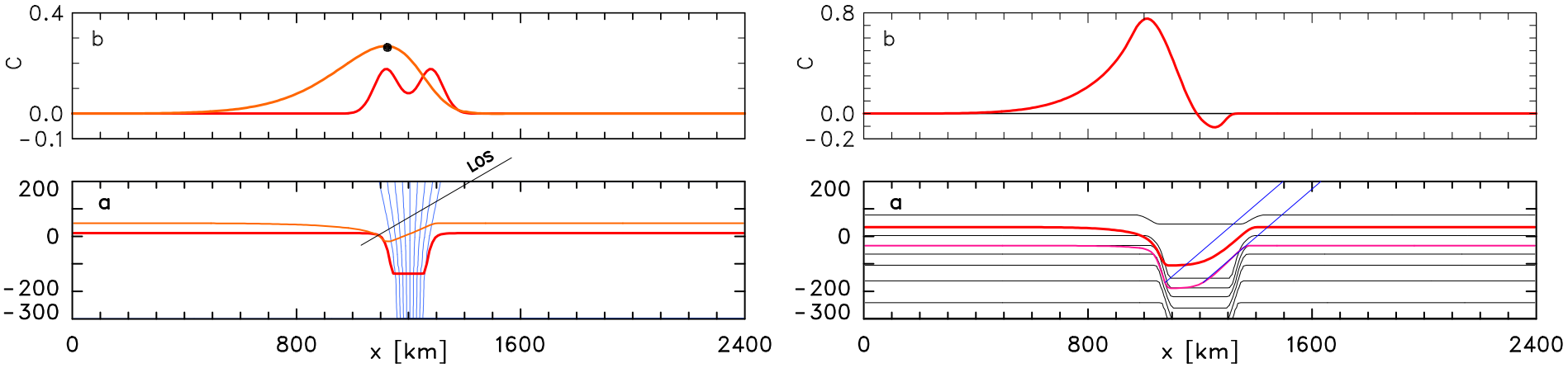

- Double humped contrast profile at disk center
- Sharp disk-center side increase due to "'hot wall"
- Gentle limbward decline at $\mu = \cos\theta = 0.5$ due to lines of sight that traverse flux sheet in photospheric layers (left of LOS)
- Contrast enhancement wider at $\mu = 0.5$ than at disk center
- Smooth distribution of polarization signal
- profiles with $30^\circ \leq \theta \leq 60^\circ$ show within a narrow region a "dark lane" centerward (in front of) the facular brightening
- Lines of sight of dark lane travel through internal atmosphere of low temperature gradient
- The dark lane is the manifestation of the "cool bottom" of faculae

Coupling magnetic field–radiation (cont

Appearance of faculae in 3-D MHD-simulations:

Center to limb variation of the G-band intensity emanating from a simulation box of 6×6 Mm at $\cos\theta = \mu = 1.0, 0.8, 0.6,$ and 0.4.

Right: Observation at $\mu = 0.63$.

From Carlsson, Stein, and Nordlund (2004) ApJL, 610, L137

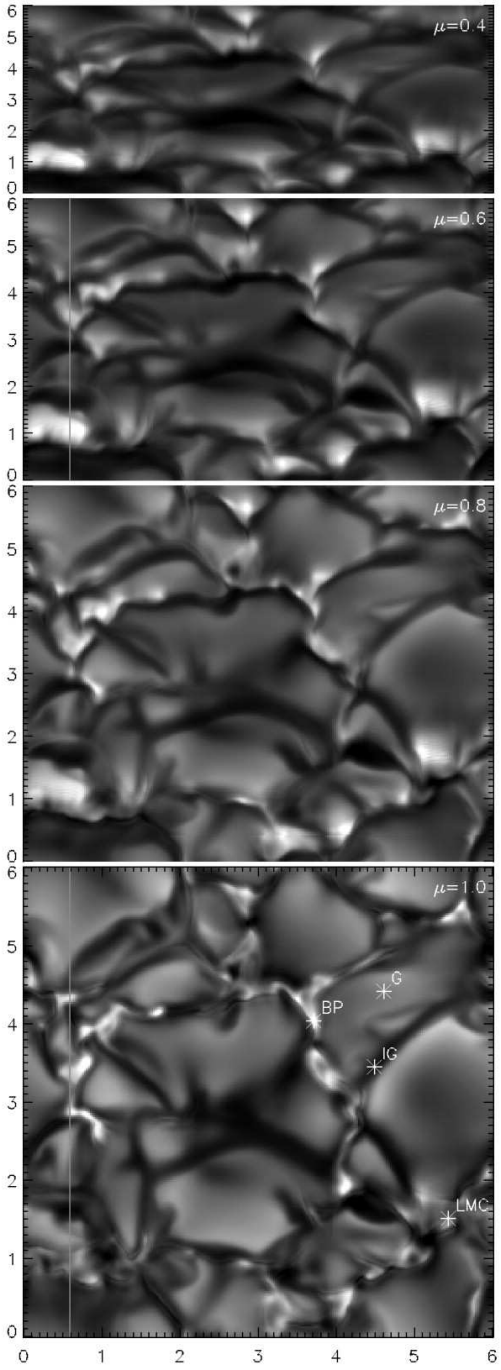

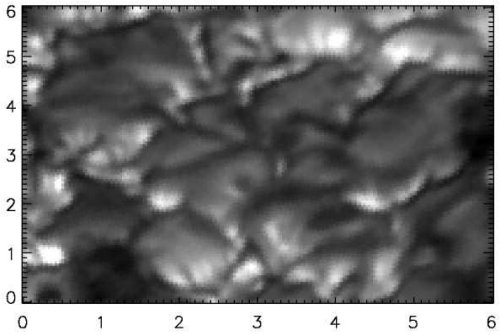

Coupling magnetic field–radiation (cont.)

Appearance of faculae in 3-D MHD-simulations:

Comparison of observed faculae (top) with faculae from the simulation box of 6×6 Mm at $\mu = 0.5$ with $\langle B \rangle = 400$ G (middle) and 200 G (bottom).

Right: Contrast profiles of facula of the middle panel (top) and the bottom panel (bottom).

Keller, Schüssler, Vögler, and Zakharov (2004) A&A 607, L59

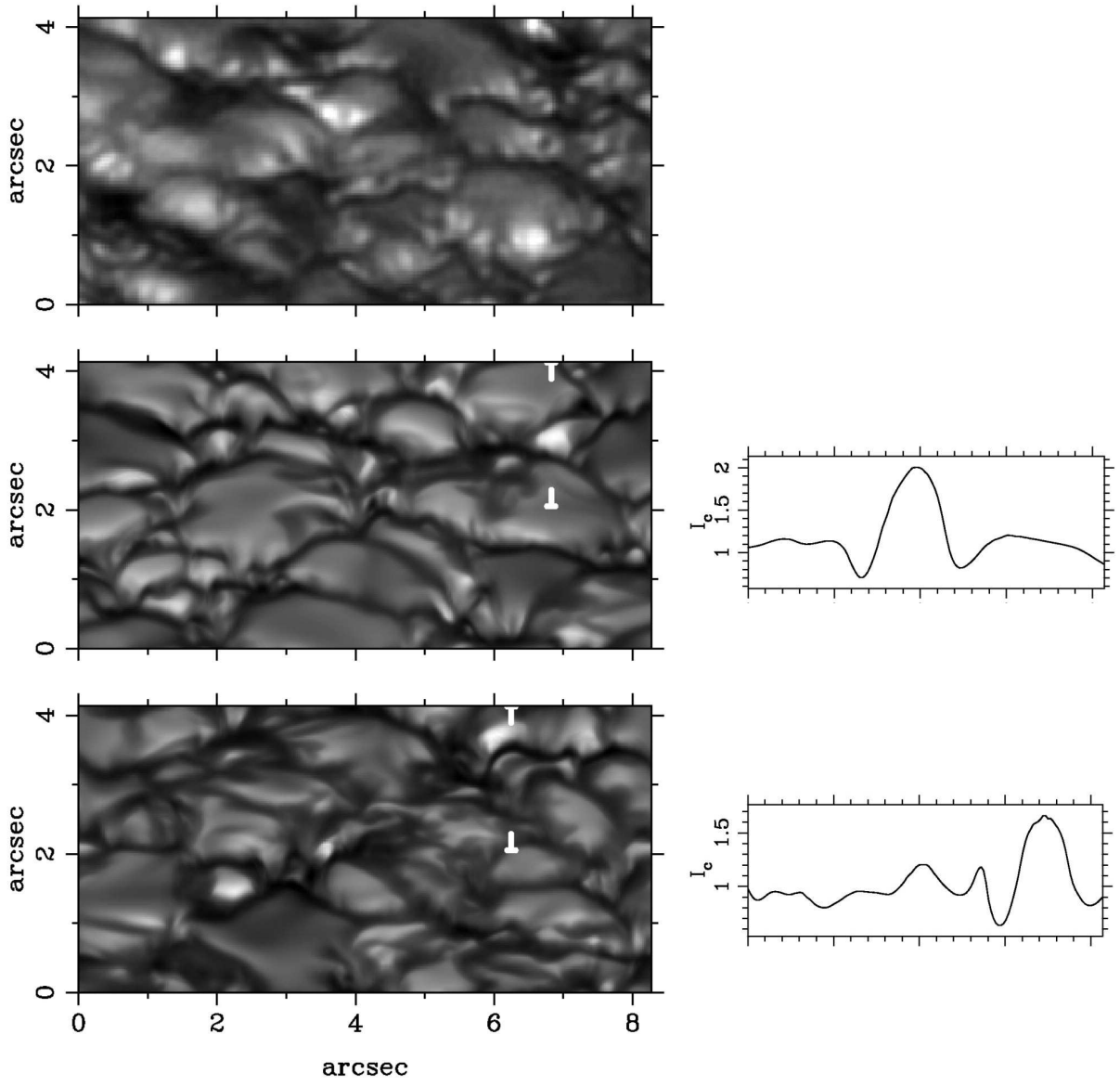

Coupling magnetic field–radiation (cont.)

Rapid temporal variability of faculae. *De Pontieu et al. (2006), ApJ 646, 1405*

"Dark bands"
in *observations* and

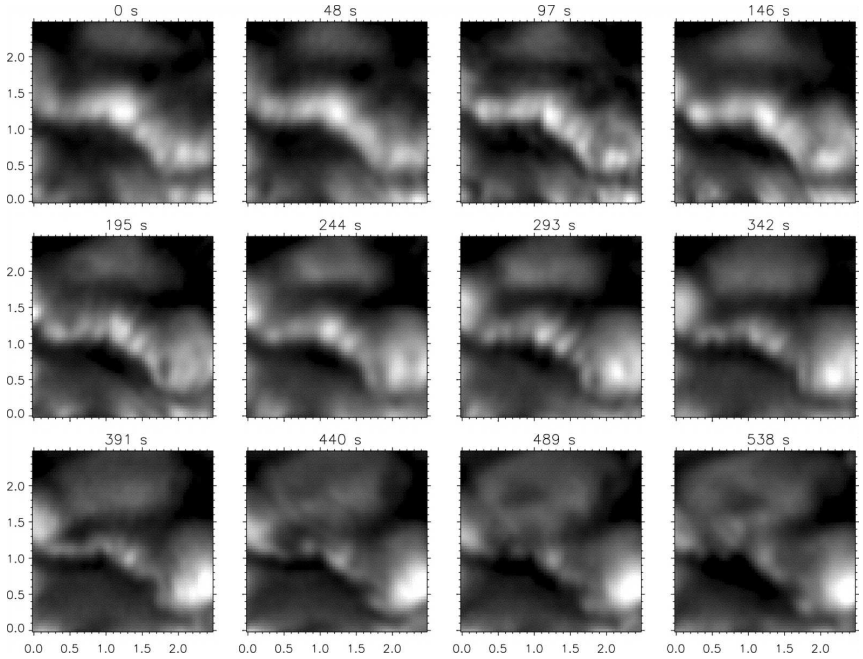

in *simulations*

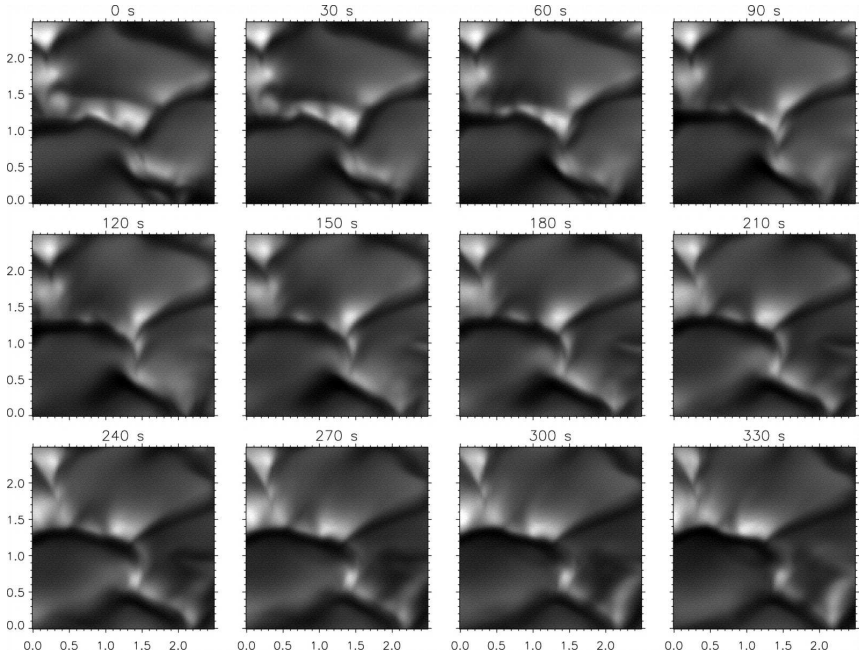

Dark bands form naturally in the course of the evolution of a granule. They correspond to the dark lane that forms when a granule is about to split, similar to the central dark region of an exploding granule.

Coupling magnetic field–radiation (cont.)

Temporal variability of facular magnetic field. Swaying flux tube?

De Pontieu et al. (2006), ApJ 646, 1405

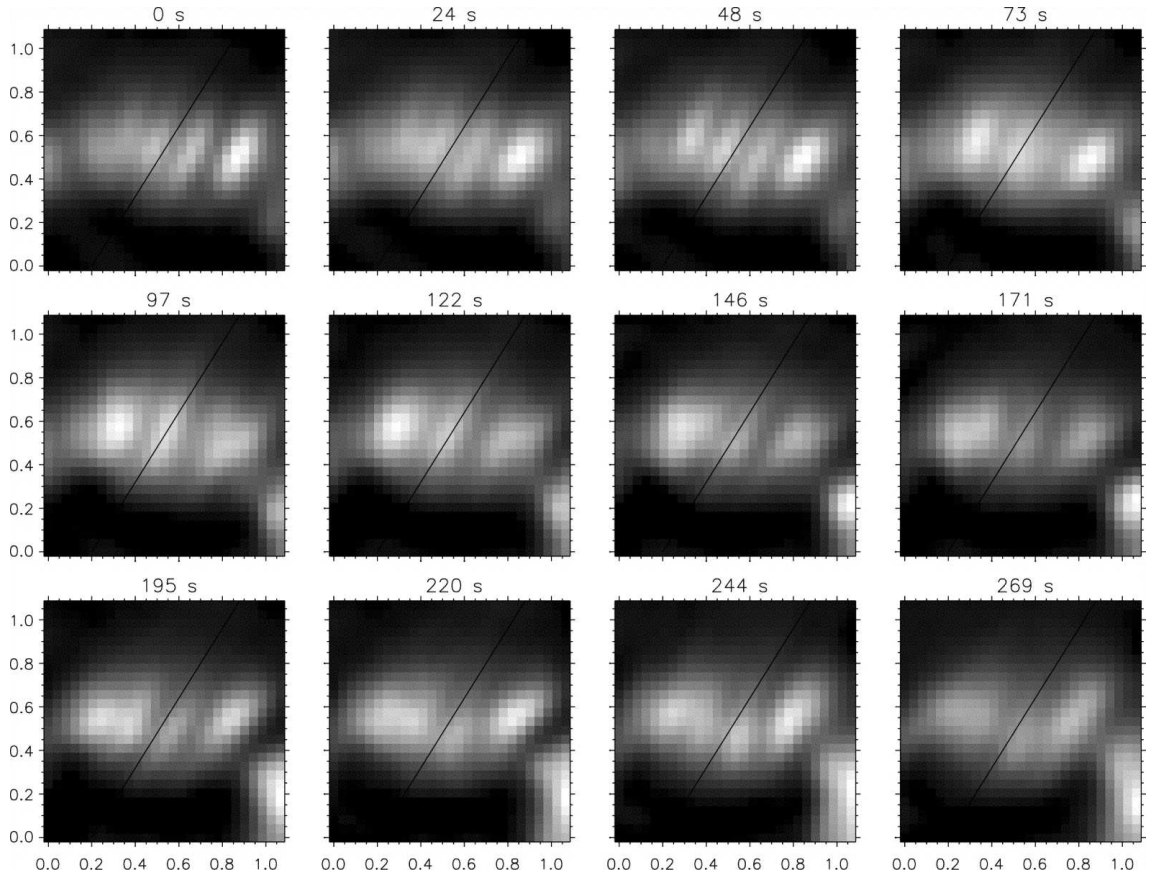

To do

- *Comprehensive model* of the center to limb variation of the brightness of faculae. Dependence on size, magnetic flux, flux density, color, etc.
- Quantitative agreement with measurements in the infrared and with measurements of the particular *geometrical displacement* of line core to continuum images of faculae or of continuum to polarization signal.
- Origin of the *striation*. Sign of interchange instability?
- Act faculae as a source of *MAG-waves*?
- *Energy balance* of faculae. Is there a surplus of radiative heat loss from faculae? How much?

Summary

- Simulations intrinsically produce a predominantly horizontally directed magnetic field in the upper photosphere.
- The horizontal field can be understood as a product of magnetic flux expulsion by the granular flow or the loopy top of the surface dynamo.
- Magneto-atmospheric waves can be used for the helioseismic mapping of the magnetic canopy in the chromosphere.
- In the “fluctosphere” magnetic field is perpetually agitated by magnetoacoustic waves and shock waves.
- The magnetic field couples to the radiation field by redirecting and channeling radiation, which produces faculae and leads to solar irradiance variation.

Table of content